EU-SCORES
European Scalable Offshore Renewable Energy Sources

European Scalable Offshore Renewable Energy Source

(EU-SCORES)

D6.2

'Renewable Coarse Resource Assessment for the European Region.'

December 2022

Delivery Date	29-11-2022
Dissemination Level	PU
Status	Final
Version	2.0
Keywords	wave energy; wind energy; resource assessment; renewable energies

Disclaimer

This deliverable reflects only the author's views and the Agency is not responsible for any use that may be made of the information contained therein.

Document Information

Grant Agreement Number	101036457
Project Acronym	EU SCORES
Work Package	WP6
Related Task(s)	Task 6.1
Deliverable	D6.2
Title	Renewable Coarse Resource Assessment for the European Region.
Author(s)	Matias Alday Gonzalez (TUD) Harish Baki (TUD) Sukanta Basu (TUD) George Lavidas (TUD)
File name	D6.2_CoarseAssessment_Final

Revision History

Revision	Date	Description	Reviewer
1	03-11-2022	Version 1	All partners
2	29-11-2022	Version 2	All partners

This project has received funding from the Europeans Union's Horizon 2020 research & innovation programme under grant agreement number 101036457.

Contents

This project has received funding from the Europeans Union's Horizon 2020 research & innovation programme under grant agreement number 101036457.

Table of Figures

This project has received funding from the Europeans Union's Horizon 2020 research & innovation programme under grant agreement number 101036457.

This project has received funding from the Europeans Union's Horizon 2020 research & innovation programme under grant agreement number 101036457.

1 Executive Summary

This Deliverable, 6.2 Renewable Coarse Resource Assessment for the European Region, aims to offer a preliminary overview of the available wind, wave and solar resources across the European Continent. The coarse assessment aims to analyse and assess the current levels of these renewable resources, analysing and discussing the expected variations per regions.

The resource assessment, even at coarse level, can indicate regions for further high resolution analysis, with better suited wind-wave-solar models. The estimated energy densities of wind, wave and solar, are partially the main indicators, we also discuss the impacts of variability, as this is expected to alter the performance of power production, when each resource is utilised by specific technologies.

This report also introduces some of the main statistical approaches and ways to estimate the resource potentials. They will be used and expanded upon in forthcoming Deliverables that will also look into power production, via coupling of high fidelity wind-wave-solar models with specific renewable converters.

Finally, in this Deliverable we discuss the role of open source coarse data and underline their limitations for operational renewable energy projects.

This project has received funding from the Europeans Union's Horizon 2020 research & innovation programme under grant agreement number 101036457.

2 Wave energy coarse assessment

The preliminary wave energy density assessment to estimate the offshore resource availability, was done using the ECMWF ERA5 reanalysis (Hersbach, et al., 2020). The ERA5 dataset was developed using the 4-dimensional (4D) data assimilation method from the Integrated Forecasting System (IFS) Cycle 41r2 and improves upon several previous iterations like the widely used ERA-Interim (Rivas & Stoffelen, 2019). The ERA5 products can be useful for preliminary analysis as they offer good temporal resolution (1 h) of sea state related variables like the significant wave height (H_s) and the peak period (T_p) or the 10 m surface wind intensities (U_{10}) and directions. However, their spatial resolution and associated shallow water physics (shoaling, refraction, bottom friction) is not suitable to perform power estimates in intermediate to shallow depth areas.

For the coarse energy density assessment we considered 30 years (from 1990 to 2020) of modelled data from the ERA5 wave product. This time window ensures that any resource estimation will also inherently consider Climate Change effects, and the variability component will be a key "hot-spot" identification. The spatial coverage selected from the wave dataset includes latitudes 30° to 69.9° North and longitudes -19° to 41.9° East, with a grid resolution (dx and dy) of 0.3°.

First, a complete characterization of the wave resource is developed based on the selected global wave product (section 2.1). Then, following a similar analysis structure, the mean wave energy estimations are presented in section 2.2.

2.1 Wave climate characterization

The wave resource analysis, for the purpose of the present study, is based on 2 wave parameters, the significant wave height (H_s) and the peak period (T_p). The characterization of these parameters is done with the mean (μ), coefficient of variation (CoV), and percentiles 95 and 99 (P_{99}, P_{95}):

Equation 1 $$\mathbf{MEAN(X) = \mu = \frac{1}{N}\sum_{i=1}^{N} X_i}$$

Equation 2 $$\boldsymbol{STD(X) = \sigma = \sqrt{\frac{1}{N}\sum_{i=1}^{N}(X_i - \mu)^2}}$$

Equation 3 $$\mathbf{CoV = \frac{\sigma}{\mu}}$$

Where X is the selected variable and N the total amount of analyzed data. The P_j percentile from a set of N ordered values in increasing order, corresponds to the smallest value from the ordered list where P percent of the data is less than or equal

This project has received funding from the Europeans Union's Horizon 2020 research & innovation programme under grant agreement number 101036457.

to P_j. CoV is non-dimensional and always ≤1. Note that the selected statistical indicators are to provide an idea of the average wave conditions, variability and extreme values.

2.1.1 Mean wave characteristics for the 30 years dataset

To provide a general view of the resource characteristics within European waters, the significant wave heights and peak periods mean and CoV are computed using the complete 30 years dataset. Additionally, we also include seasonal characterization of wave parameters to provide an idea of the average conditions during winter (DJF), spring (MAM), summer (JJA) and autumn (SON)[1]. The analysis is centered on mainly 4 zones:

- Portugal: Between latitudes 36.5° and 42.0° N, and up to longitude 10° W.
- Ireland: Covering only the Atlantic coast, from latitudes 51° to 55.5° N and up to longitude 11° W.
- Scotland: Including the north coast and Atlantic exposed coasts of the Orkneys and the Hebrides. Basically between latitudes 56.7° and 59.9° N.
- North Sea: Mainly off the coasts of Belgium, The Netherlands and Germany, covering longitudes 2.5° to 8.25° E.

Given the coarse spatial resolution of the ERA5 wave product grid, the overall analysis is done considering data from a distance ≥ ~0.25° (30 km approx.) from the coastlines. These zones and considerations also apply for the analysis presented in section 2.2.

In Figure 1 is possible to observe that off the coasts of Portugal the mean wave climate presents H_s close to 2.3 m and T_p normally close to 11 s. While mean T_p values are similar within the Bay of Biscay, there is a slight reduction on the mean wave height conditions with H_s of the order of 2.0 m (or smaller).

The west coast of Ireland stands out as a highly energetic area, exposed to Hs of about 3 m offshore and averaged peak periods larger than 10.5 s. Alike conditions are observed in the Northern coasts of Scotland and West coasts of The Orkneys with an apparent reduction of the wave heights. The latter effect could be attributed to the coarse spatial resolution of the ERA5 model, which does not allow to properly solve some bathymetry features

[1] DJF = December-January-February, MAM = March-April-May, JJA = June-July-August, and SON = September-October-November.

This project has received funding from the Europeans Union's Horizon 2020 research & innovation programme under grant agreement number 101036457.

nor the complex coastlines in this area affecting wave propagation.

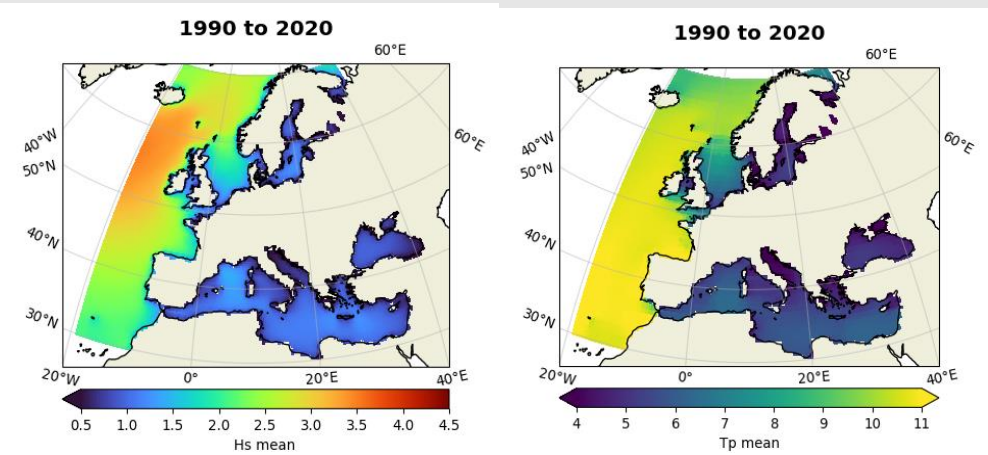

Figure 1. 30 years mean H_s and T_p values from ERA5 reanalysis.
Colorbar on left panel indicates H_s values in meters, colorbar on right panel indicates T_p in seconds.

The North Sea is mildly exposed to swells radiated from the North Atlantic at high latitudes (roughly around 60° North), an effect more noticeable along the Southwest fjords of Norway. There is also a seasonal influence of swells propagating from the Norwegian Sea to the South. The combined effect of these elements explains the slightly higher mean T_p between latitudes ~58° to ~62° (of about 9 s). Otherwise, wave conditions within the North Sea are mostly driven by local winds which together with a relatively short fetch for wave generation, result in smaller mean peak periods (~6 to ~8 s). Additionally, due to the reduced depths, wave propagation is highly affected by bottom friction effects which should be carefully considered in the wave model to avoid under/over estimation of wave heights (Alday, et al., 2022) (Guillou, 2014).

The seasonal average for the 30 years period shows the expected overall increase of wave heights and periods along the Atlantic coasts (from Portugal to Scotland) and the North Sea (Figure 2., DJF panels). Particularly large wave heights are observed off the coasts of Ireland and Scotland with DJF means >5 m. The largest mean T_p for winter (DJF) are found south of Portugal, reaching values close to 13 s. Similar values are found along Ireland and Scotland (~12 s), and ~6 to 7 s along the south coasts of the North Sea.

We notice an important reduction of H_s and T_p for summer months (JJA) for all analyzed locations; About ~2 m offshore Ireland and Scotland, ~1.7 in average off the coasts of Portugal and ranging from 0.8 to 1 m in the North Sea between Belgium and Germany.

Especially short periods off the Dutch coast and Belgium with values of the order of 5.5 s (these values increase slightly to

This project has received funding from the Europeans Union's Horizon 2020 research & innovation programme under grant agreement number 101036457.

~6.0 s or 6.5 s during NAM and SON). For the coasts exposed to the Atlantic the JJA T_p mean values range from 8 to 9 s (Figure 2., JJA panels).

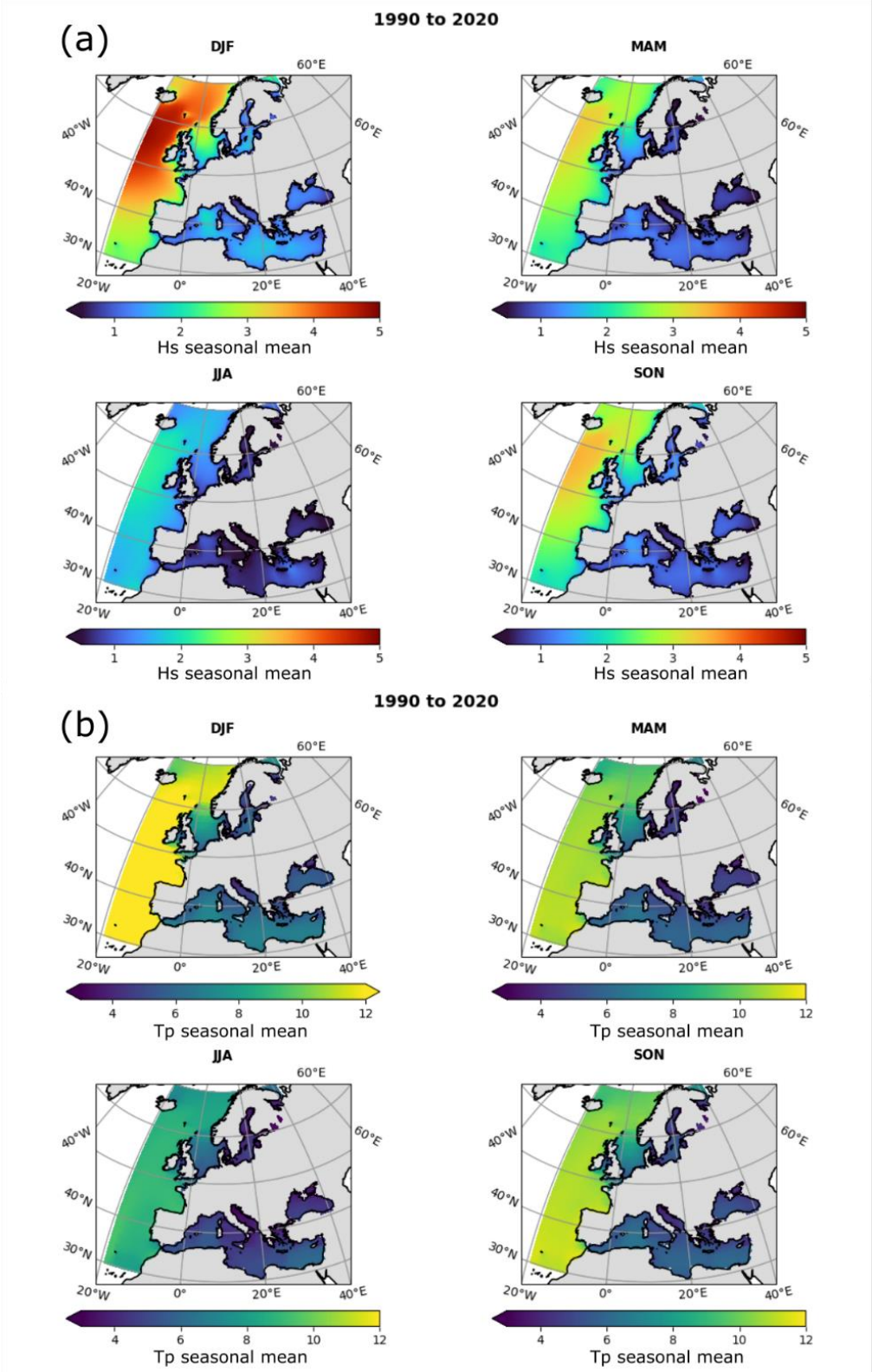

Figure 2. (a) H_s and (b) T_p seasonal means for the 30 years period.
Colorbar on (a) indicates significant wave height (H_s) values in meters. Colorbar on (b) indicates peak period (T_p) values in seconds.

This project has received funding from the Europeans Union's Horizon 2020 research & innovation programme under grant agreement number 101036457.

The coefficient of variability (CoV) computed for the full dataset provides an idea of the dispersion of the wave parameters. In Figure 3. is possible to observe that, overall, wave heights present larger values of CoV than peak periods, being especially high (>0.6) in those areas where wave conditions are mostly driven by local winds (local wave generation). These areas are mainly the Mediterranean Sea, The Baltics, and most important in the context of this study, The North Sea.

Notice that Portugal presents a relatively low CoV, most likely due to a swell dominated wave climate, less influenced by the locally generated waves. The CoV of T_p are considerably lower than for H_s, with overall values <0.4. We note that most areas with higher CoV values (>0.4) are located near the coast, which could be related to spurious variability of the wave fields in shallower regions that are not properly solved by the model. This could also be due to inaccuracies of the modelled atmospheric boundary layer development as it transitions from water to land (or the opposite) and thus affecting the wind values used to force the wave model (Ardhuin, et al., 2007; Dobson, et al., 1989).

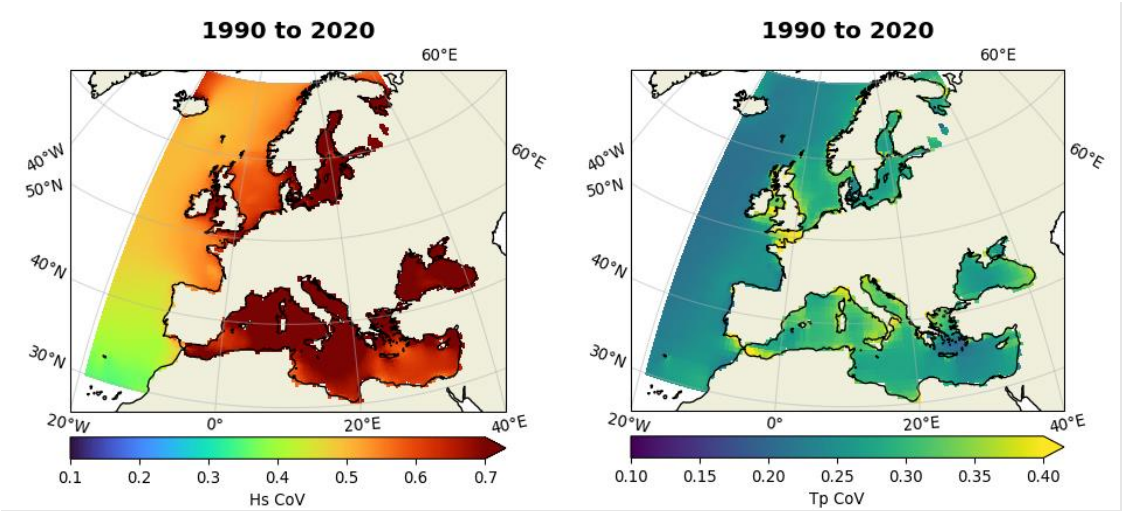

Figure 3. Coefficient of variation computed over 30 years for significant wave height (H_s) and peak period (T_p).
Colorbars on left and right panel indicate CoV for wave height in meters and peak period in seconds respectively.

2.1.2 Wave field variability

The mean values presented in section 2.1.1 give a general overview of the resource availability within the analyzed area. To provide further details on the wave fields' variability in time, we have developed a similar statistical analysis for yearly data. In this case we have identified the years with mean H_s clearly below the total 30 years mean, and those years which stand out for their higher wave heights.

This project has received funding from the Europeans Union's Horizon 2020 research & innovation programme under grant agreement number 101036457.

Characterization of these higher/lower energy years is done with the normalized difference of the yearly mean with respect to the 30 years mean (not shown). Finally, a few examples of seasonal variability are provided to characterize wave field changes during winter ,spring), summer and autumn from a couple of the identified higher/lower energy years. The aim of this brief analysis is to quantify the variability of the wave field characteristics, and its outcome can provides an idea of upper and lower bound mean values of H_s and T_p within the areas of interest.

The identification of the years characterized as "low energy years" is based on the mean yearly significant wave values. We must highlight that the magnitude of the "deviations" from the 30 years mean is not constant at each location (Portugal, Ireland, North Sea, etc.). More detailed local studies will be carried out throughout EU-SCORES to properly assess inter annual variability and its potential link to atmospheric oscillation indicators. As seen in Figure 4 and Figure 5, a total of 6 years were identified from the 30 year dataset following the process described above. The selected years were considered to be the most representative of overall mean yearly wave heights below the 30 year mean (Figure 1).

Years 1991, 2003 and 2012 present yearly mean H_s that are slightly below the 30 years mean. Still we identified wave mean height reductions that can be close to 8% off the coasts of Portugal, >6% along Ireland and Northern Scotland and >10% at the North Sea. For these years the peak periods changes are smaller along the coasts exposed to North Atlantic swells (

Figure 5). With mean reductions of about 2% offshore Portugal, ~4% reduction along Ireland and Scotland. On the other hand mean T_p reduction can be larger than 5% in the North Sea compared to the 30 years average.

Mean wave height reductions are more noticeable for years 1996, 2001 and 2010 (Figure 4). Although for these years wave heights off the coast of Portugal are less affected and even a bit higher than the 30 years mean (~5% higher in 1996). Largest mean H_s reductions (~15%) are observed within the Bay of Biscay and along the coasts of Ireland and Scotland. In the North Sea, wave height reductions (compared to the 30 year mean) are more variable, but overall they are close to 7%. Peak period mean reductions can be of about 3 to 5% in Portugal and Ireland, slightly higher (~7%) at the Bay of Biscay and more variable at the North Sea.

This project has received funding from the Europeans Union's Horizon 2020 research & innovation programme under grant agreement number 101036457.

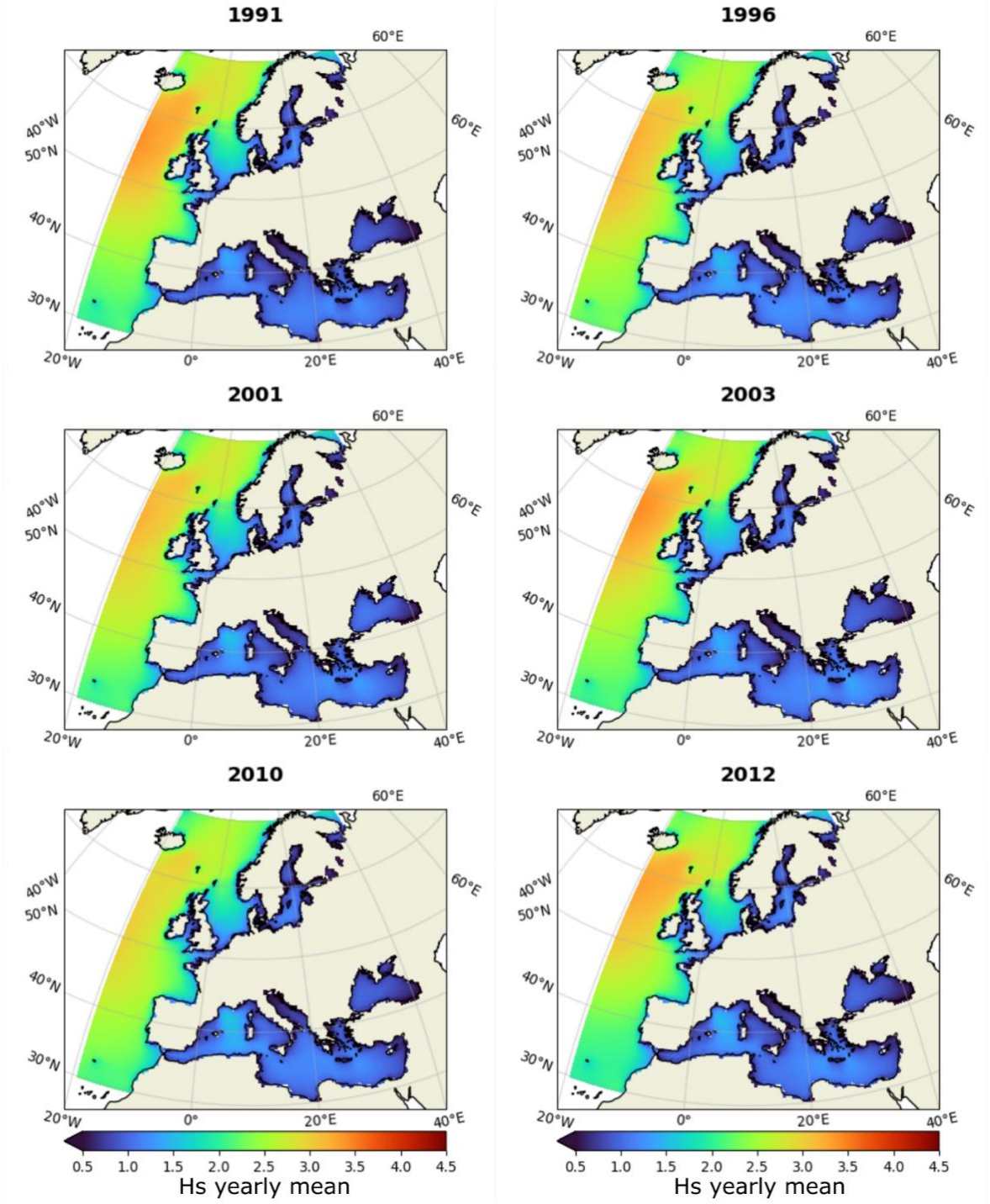

Figure 4. Significant wave height (H_s) yearly mean from selected low energy years. Colorbar indicates significant wave height values in meters.

This project has received funding from the Europeans Union's Horizon 2020 research & innovation programme under grant agreement number 101036457.

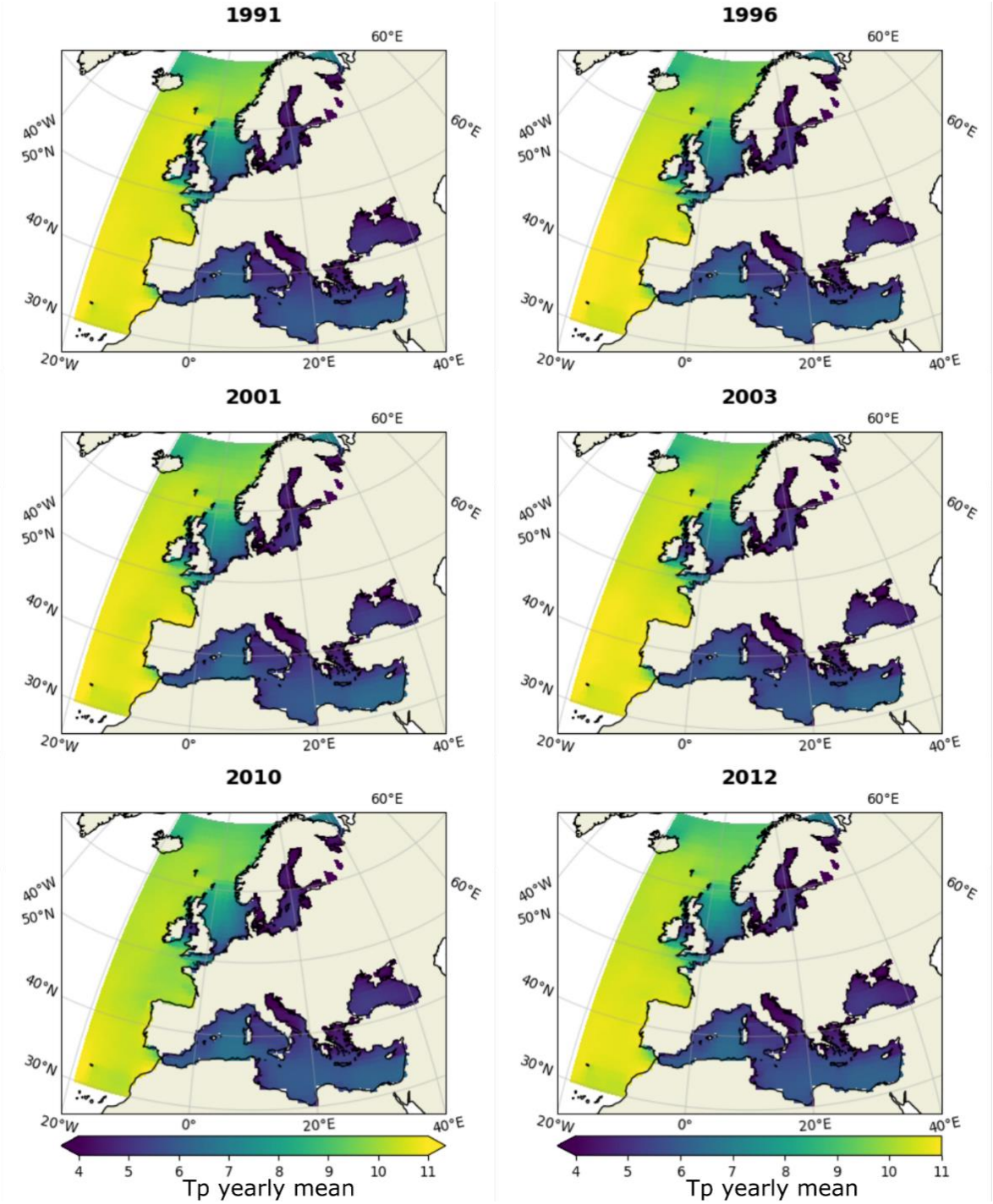

Figure 5. Peak period (T_p) yearly mean from selected low energy years. Colorbar indicates peak period values in seconds.

In Figure 6 we present those years that stand out for their higher mean significant wave heights. In general the larger Hs differences are identified off the Atlantic coasts of Ireland and Scotland, with wave heights yearly means at least 10% higher than the full dataset mean. Identified "deviations" of wave conditions offshore Portugal are less profound, with Hs yearly means that can be ~5% higher than the 30 years mean. At the

This project has received funding from the Europeans Union's Horizon 2020 research & innovation programme under grant agreement number 101036457.

North Sea once again the changes are more variable, but in general is observed an Hs increase of ~5% that for these years.

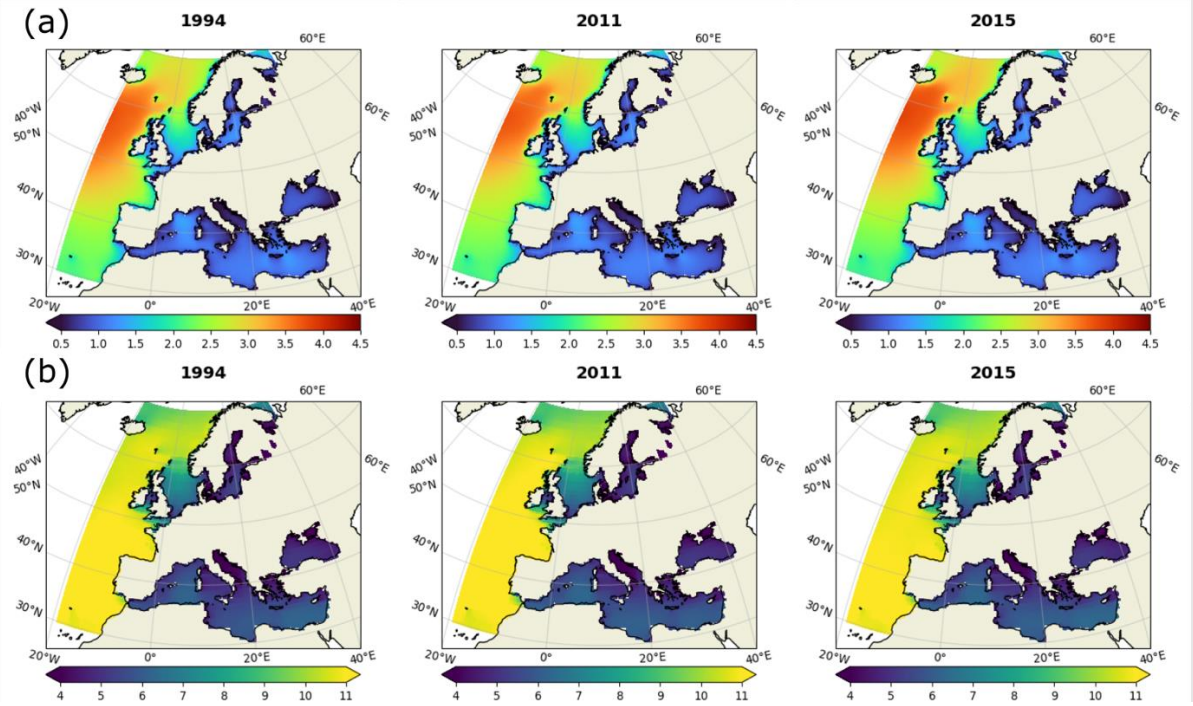

Figure 6. Identified high energy years. (a) yearly mean H_s and (b) yearly men T_p.
Colorbar on (a) indicates significant wave height values in meters. Colorbar on (b) indicates peak period values in seconds.

For the "high" energy years , changes of the mean peak period are considered not significant, being typically 2.5% higher at Portugal, and the Atlantic coasts of Ireland and Scotland (Figure 6b).

Two years were chosen to illustrate the seasonal changes of the wave field 2001 (Figure 7) and 2015 (Figure 8). These correspond to the years with the smallest and largest yearly mean H_s respectively. Note how the largest seasonal changes in wave height and peak periods occur at high latitudes (>45°; off the coasts of Ireland and Scotland). These results are in line with the previous CoV results obtained from the general analysis (Figure 3.). It is also possible to see how the winter (DJF) and spring (MAM) of 2015 had particularly large waves (Figure 8). While largest changes in the wave field's T_p are observed in the North Atlantic (form ~9 to >12 s), the North Sea seems to be less affected by seasonal changes, probably due to its fetch characteristics. Although, there is still a clear variability on wave heights.

This project has received funding from the Europeans Union's Horizon 2020 research & innovation programme under grant agreement number 101036457.

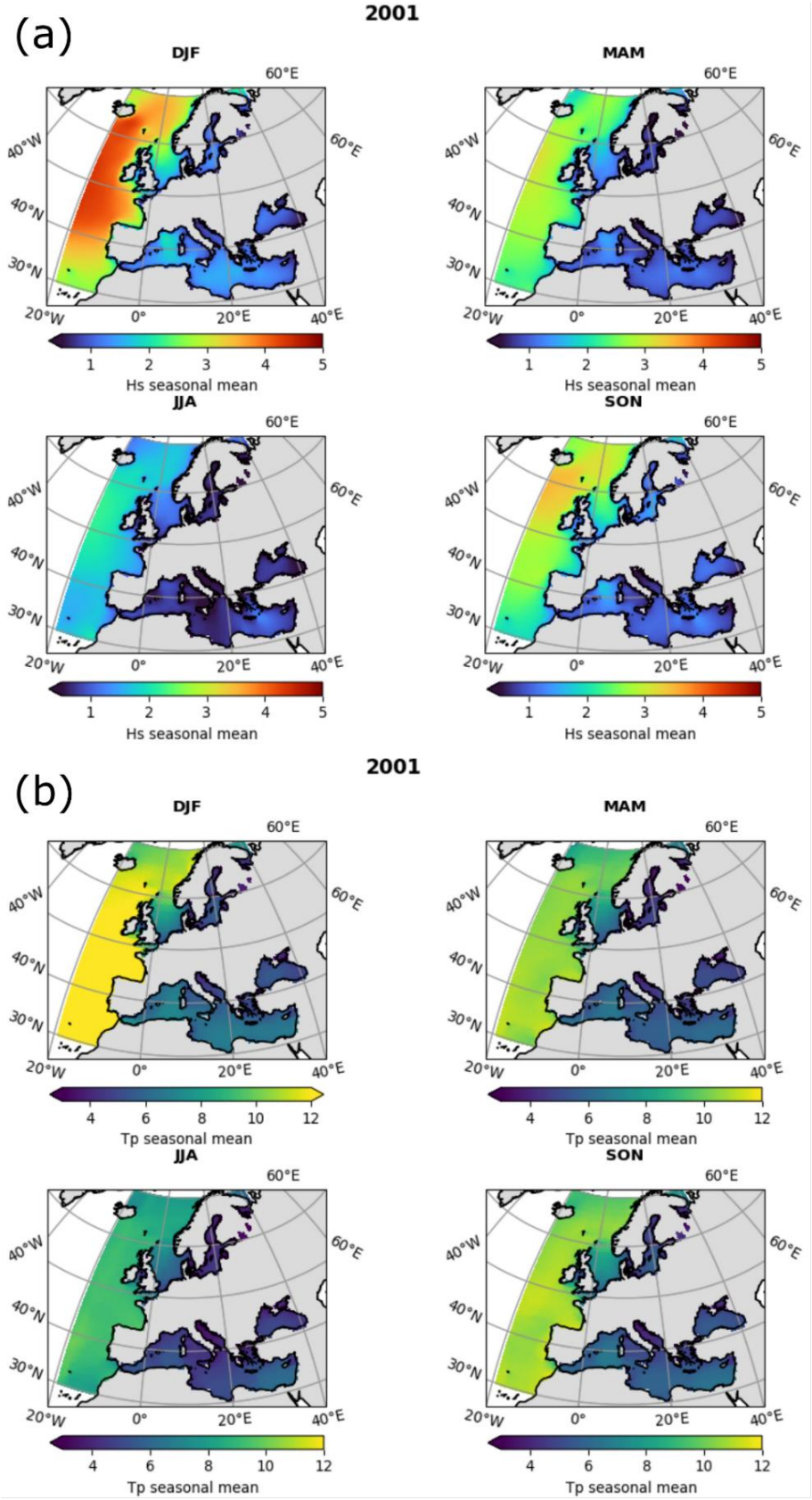

Figure 7. (a) H_s and (b) T_p seasonal means for year 2001.

Colorbar on (a) indicates significant wave height (H_s) values in meters. Colorbar on (b) indicates peak period (T_p) values in seconds.

This project has received funding from the Europeans Union's Horizon 2020 research & innovation programme under grant agreement number 101036457.

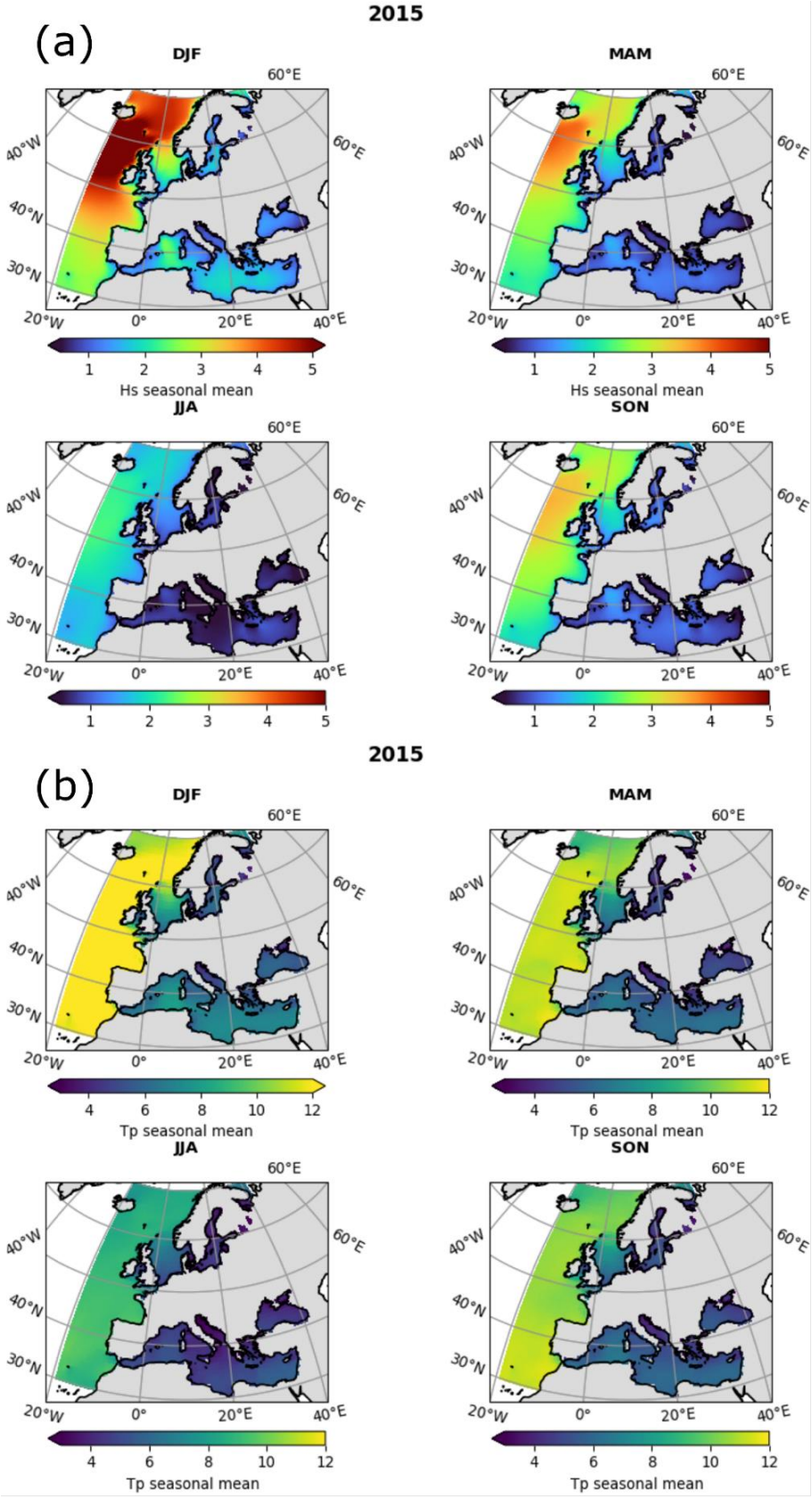

Figure 8. (a) H_s and (b) T_p seasonal means for year 2015.

Colorbar on (a) indicates wave height values in meters. Colorbar on (b) indicates peak period values in seconds.

This project has received funding from the Europeans Union's Horizon 2020 research & innovation programme under grant agreement number 101036457.

2.1.3 Overview of extreme conditions

The significant wave heights' percentile 95 and 99 (P_{95} and P_{99}) have been computed for the identified years with higher yearly H_s mean (1994, 2011 and 2015). Although these values provide a good idea of the extreme wave conditions, they should not be used for design purposes, but they can be considered as a reference for operation conditions under strong weather. Additionally, the strongest storms do not necessarily occur within the years with higher mean H_s.

P_{95} shows similar wave height values for the 3 selected years, with H_s >6 m offshore the Atlantic coasts of Ireland and Scotland and >4 m at Portugal (Figure 9a). The P_{99} of H_s shows the sea states with the highest wave height simulated for each year at any given grid node of the ERA5 wave model (Figure 9b). The year 1994 presents particularly large values at all locations along the Atlantic European coasts, with waves offshore Ireland >10 m.

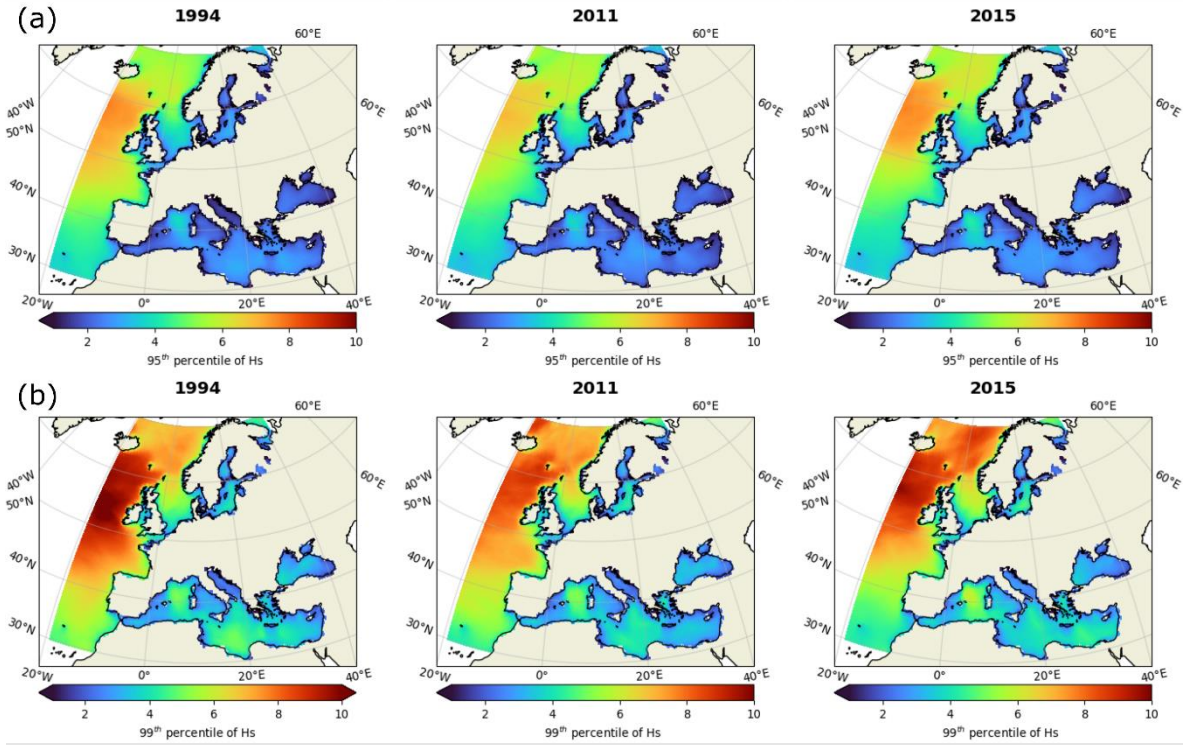

Figure 9. (a) H_s 95th percentile and (b) H_s 99th percentile for years 1994, 2011 and 2015.

Colorbars indicate significant wave height values in meters.

2.2 Wave energy assessment

The wave resource assessment developed in section 2.1 provides a general description of the sea states' characteristics in terms of significant wave heights and peak periods. These parameters were obtained from a coarse spatial resolution model

This project has received funding from the Europeans Union's Horizon 2020 research & innovation programme under grant agreement number 101036457.

which better represent wave conditions in deep to intermediate water depths. In the present section, H_s and T_p values from the ERA5 wave product are used to compute the wave power density per meter (pWave).

The power density is computed with the following expression, valid for deep waters:

Equation 4 $$\mathbf{pWave = \frac{\rho_w}{64\pi}(gH_s)^2T_e}$$

In Equation 4, ρ_w is the sea water density, here taken as 1026 kg/m3, g is the acceleration of gravity (9.8 m/s), H_s the significant wave height in m, and T_e the wave energy period (s) here estimated as $0.9T_p$ as see in (Lavidas & Vengatesan, 2018). However, it is important to note that the conversion factor of T_p will depend on regional characteristics (Guillou, et al., 2020).

Similar to the statistical characterization of the wave climate done in section 2.1, in the following subsections we present a description of the wave energy resource. The wave power is based on the deep water equation as the components sources from ERA5, that are bulk parameters and not spectral information that can provide higher accuracy. A briefing of the power density estimations is then presented in section 2.3.

2.2.1 30 years mean wave power (1990 to 2020)

The pWave mean and CoV computed for the complete dataset is presented in Figure 10. To facilitate the visualization of pWave gradients within the analyzed domain we have saturated the plot levels to 50 kW/m in Figure 10a, but the total wave power mean offshore Ireland and Scotland is estimated to be close to 56 kW/m, and between 30 to 35 in kW/m Portugal (depending on the latitude). There is a clear latitudinal variation at the North Sea. Off the coast of the Netherlands the total mean does vary from 6 to ~10 kW/m from West (close to Belgium) to East (reaching Germany).

The lowest coefficient of variation is estimated at Portugal, with values typically of 1.2. This lower CoV if probably due to the influence of longer (distant) swells propagating from the West and West-South-West. On the other hand the slightly higher CoV values found along Ireland and Scotland (between 1.2 and 1.4) are related to their higher exposure to North Atlantic storms. As expected, and from what it was already seen on the wave field analysis (Figure 3.), the highest CoV values (from the studied locations) are found along the Southern North Sea, with values between 1.6 and 1.8 (Figure 10b).

This project has received funding from the Europeans Union's Horizon 2020 research & innovation programme under grant agreement number 101036457.

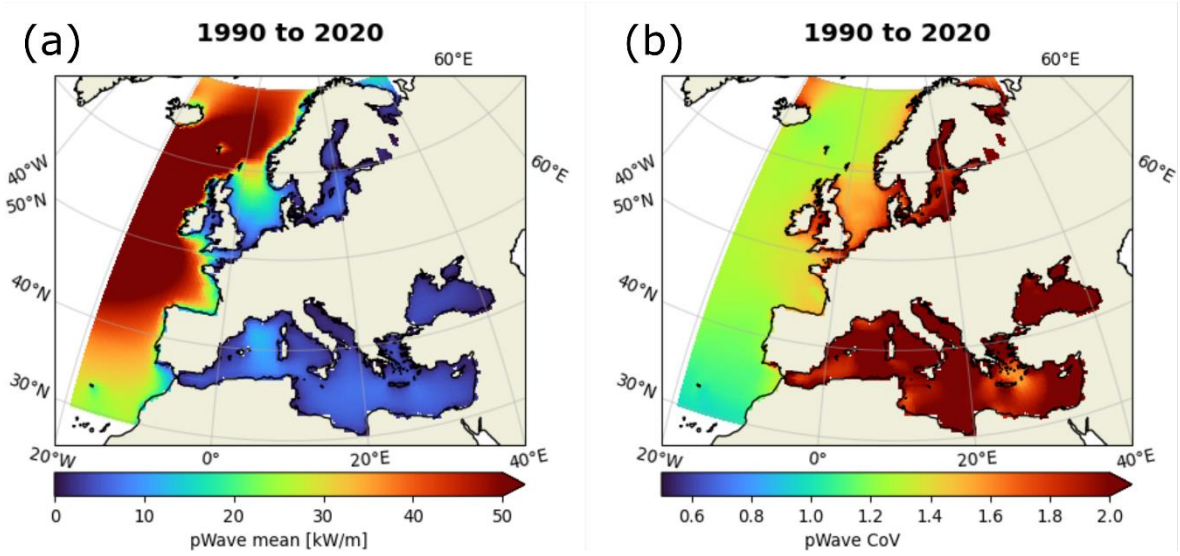

Figure 10. (a)Mean wave energy density and (b) Total pWave CoV estimated for full dataset (1990 to 2020).

Colorbar in (a) indicates wave power density in kW/m. Colorbar in (b) indicates coefficient of variation levels.

Similar to what was done in section 2.1.1, a seasonal mean of the complete dataset (30 years) is included to further describe the wave resource availability (Figure 11). While autumn (MAM) and spring (SON) average conditions are similar to the total 30-year pWave mean presented in Figure 10a, DJF and JJA means largely differ. For example, the 30-years JJA pWave mean off the coasts of Portugal ranges from ~10 to ~12 kW/m and can reach values from 50 to 65 kW/m (from South to North) during summer (DJF), about 5 times larger than in JJA. Changes that can be even more pronounced for Ireland, with JJA mean pWave of about 110 kW/m and approx. 15 kW/m during DJF. In some places along the coast the DJF/JJA pWave ratio can be of the order of 10 (this should be verified with a high resolution model).In Scotland, off the Atlantic coast of the Hebrides the mean DJF pWave can be >100 kW/m, and ~80 kW/m at the Orkneys. These values drop to ~16 and ~10 kW/m for the 30-year mean JJA at the same places respectively. For the North Sea, it can be said that the wave resource during DJF (≥10 kW/m) is about 3 times the mean pWave during JJA (~3 kW/m averaged from Belgium to Germany).

This project has received funding from the Europeans Union's Horizon 2020 research & innovation programme under grant agreement number 101036457.

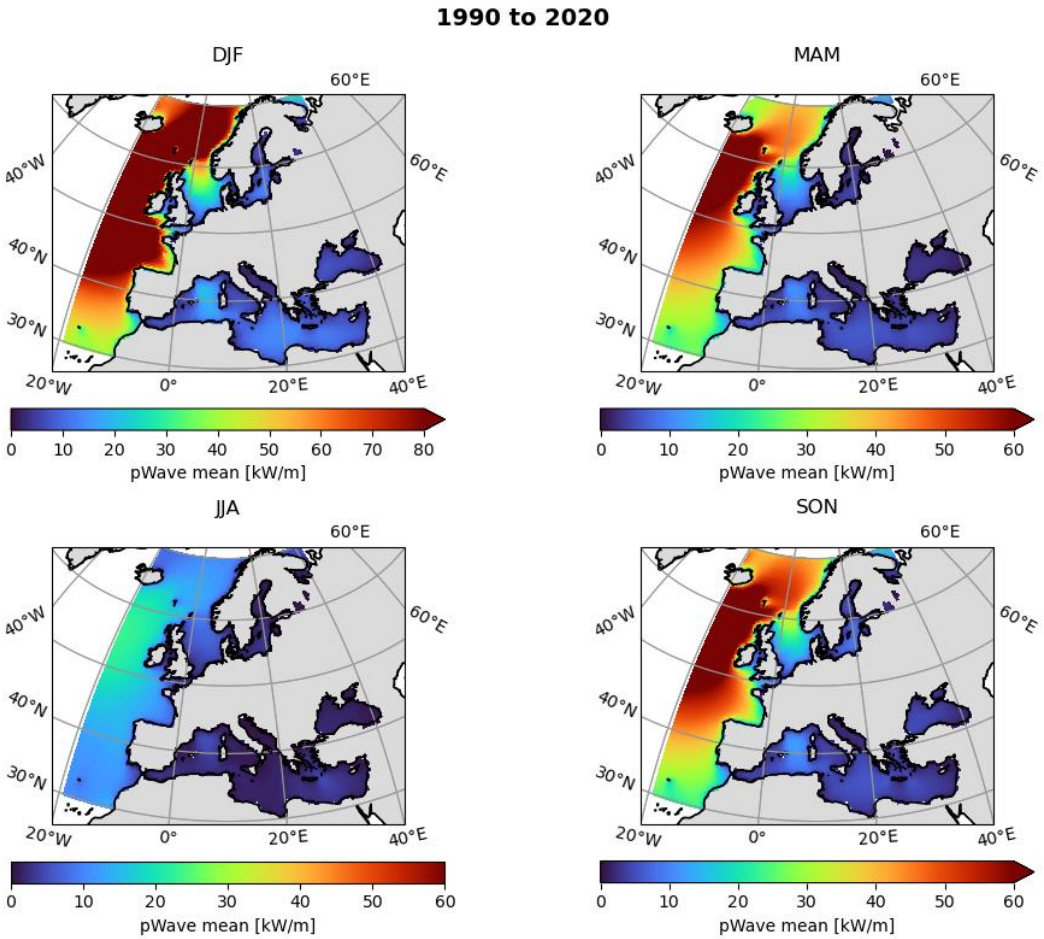

Figure 11. Wave power density seasonal 30 years mean.

This project has received funding from the Europeans Union's Horizon 2020 research & innovation programme under grant agreement number 101036457.

2.2.2 Wave resource variability

As seen in section 2.1.2, there are yearly mean values that clearly deviate from the mean wave heights and peak periods with full dataset 30 years mean(

Figure 5, Figure 6). Note that since the expression of the wave power density is function of Hs to the second power, changes of the wave heights have a larger impact on pWave compared to changes of the peak period. Here we present an overview of the yearly mean pWave estimation for those years previously identified with yearly mean Hs lower and higher than the 30 years total mean (Figure 12).

Among the lower energy years, 2001 and 2010 stand out for their considerably low mean pWave levels, particularly offshore Ireland and Scotland. The 2010 mean power density at these locations is in average ~35 and 37 kW/m respectively (over 20 kW/m lower than the 30 years mean; see Figure 10), while the 2001 mean is close to 40 kW/m. Within Portuguese waters these changes are less dramatic, with mean pWave ranging from 25 to ~29 kW/m in 2010, and from about 27 to ~32 kW/m in 2001 (always with higher energy levels along the Northern coast of Portugal, Figure 12a).

For the 3 "high" energy years identified, 1994 shows especially high mean pWave values offshore Portugal ranging from ~33 to ~43 kW/m (in average ~6 kW/m higher than the 30 year mean). Although 2015 presents overall high power density levels for higher latitudes (e.g. >45°), this intensification is only mild within Portuguese waters. Mean pWave values of ~29 to ~36 kW/m are basically the same as the total 30 years mean. This later effect is thought to be related to the directionality of the wave fields propagating to the coast, a factor that should be further analyzed specially to assess its effect in shallower depths with higher resolution models.

The mean pWave values for 2015 are particularly high offshore Ireland, reaching ~73 kW/m (and higher) along the northern coast and about 70 kW/m south of Galway. Similar values are observed off the coast of the Hebrides in Scotland (~70 kW/m), and about 60 kW/m offshore the Orkneys.

This project has received funding from the Europeans Union's Horizon 2020 research & innovation programme under grant agreement number 101036457.

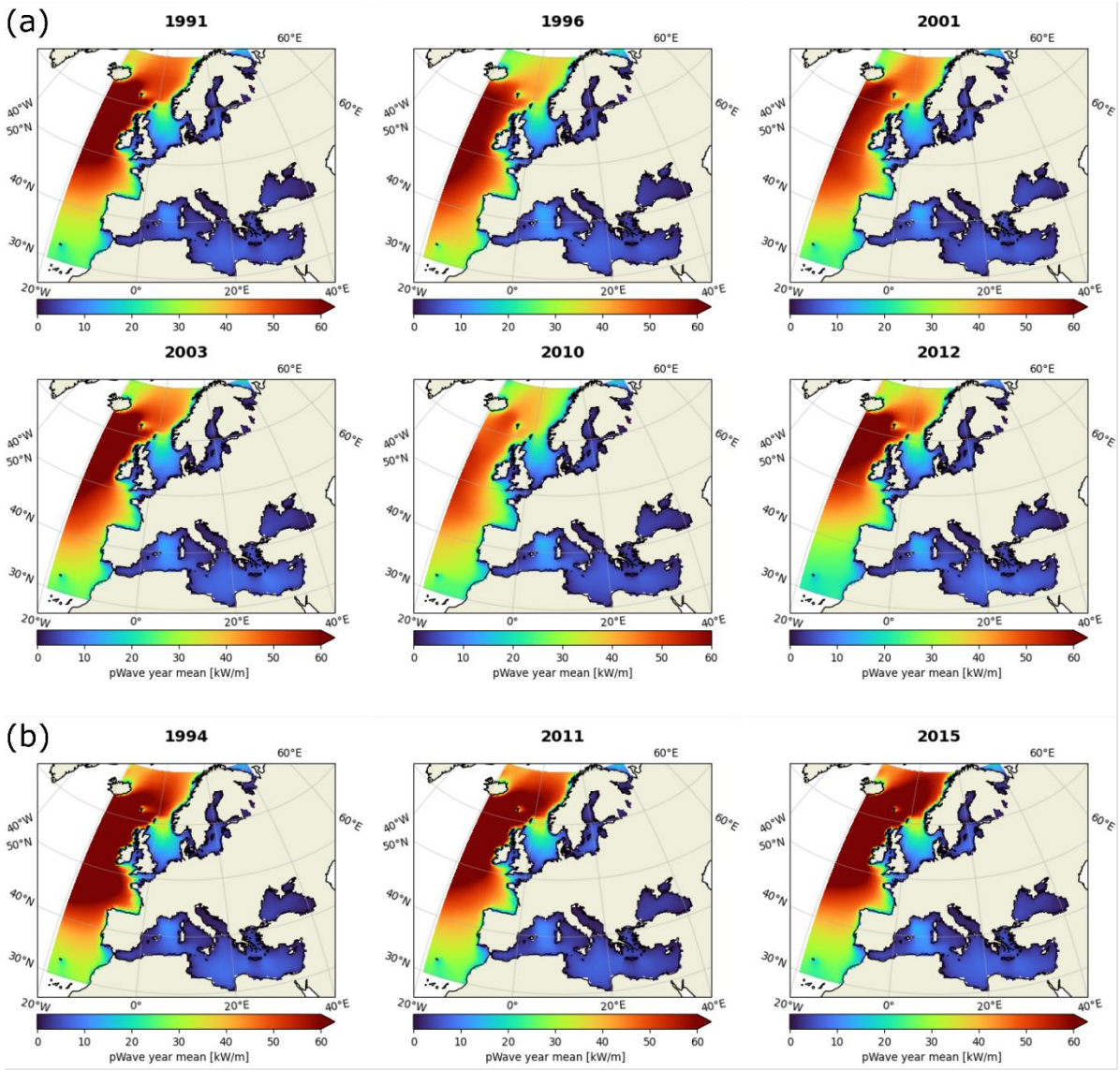

Figure 12. Yearly mean pWave for (a) identified lower energy years and (b) high energy years.

Colorbars indicates wave power density in kW/m.

2.3 Wave resource coarse assessment briefing

A complete results' briefing is presented in Table 1. The table condenses the offshore mean power wave density values estimated from the ERA5 wave model for the complete 30 year dataset and for those year with overall higher and lower mean wave height values. As previously described, 4 main areas were included: Portugal, Ireland, Scotland, and the North Sea.

This project has received funding from the Europeans Union's Horizon 2020 research & innovation programme under grant agreement number 101036457.

Table 1. Coarse wave resource assessment results' briefing.

North Sea covers eastern Belgium to Germany. Values provided for Scotland are an estimated mean offshore value for the Hebrides and Orkney.
Values in red show the highest mean pWave estimated.

Period/Year	Location	Mean pWave [kW/m]	Comments
1990 - 2020	Portugal	30 to 35	pWave increasing to the North
	Ireland	52 to 56	pWave increasing to the North
	Scotland	54 And 46	pWave at Hebrides and Orkney
	North Sea	4 to 9	pWave increasing to the East
1994 (High energy year)	Portugal	33 to 43	pWave increasing to the North
	Ireland	65 to 70	pWave increasing to the North
	Scotland	60 and 55	pWave at Hebrides and Orkney
	North Sea	4.5 to 9	pWave increasing to the East
2011 (High energy year)	Portugal	29 to 36.5	Higher mean pWave at Northern regions
	Ireland	59 to 65	Offshore pWave increasing at Northern regions
	Scotland	59 and 51	pWave Hebrides and Orkney
	North Sea	3.5 to 9.5	pWave increasing Eastwards
2015 (High energy year)	Portugal	29 to 36	Offshore pWave increasing to the North
	Ireland	68 to 73	pWave increasing at Northern regions
	Scotland	70 and 60	the Hebrides and Orkney
	North Sea	4 to 10	pWave increasing to the East
1991 (Lower energy year)	Portugal	27 to 30	pWave increasing to the North
	Ireland	57 to 58	Highest mean (~60) found at latitude 53.3° approx.
	Scotland	53 and 44	Hebrides and Orkney. pWave decreases to the North of the Hebrides
	North Sea	4 to 9.5	pWave increasing to the East
1996 (Lower energy year)	Portugal	30 to 35	pWave increasing to the North
	Ireland	45 to 43	pWave is very homogeneous North to South
	Scotland	40 and 32	the Hebrides and Orkney
	North Sea	4 to 8	pWave increasing to the East
2001 (Lower energy year)	Portugal	27 to 32	pWave increasing to the North
	Ireland	38 to 40	pWave increasing to the North
	Scotland	38	Similar offshore the Hebrides and Orkney
	North Sea	4.5 to 9	pWave increasing to the East
2003 (Lower energy year)	Portugal	30 to 35	pWave increasing to the North
	Ireland	50 to 54	Similar from North to South
	Scotland	50 and 40	Hebrides and Orkney. Slightly decreasing to the North at the Hebrides.
	North Sea	3.5 to 7.5	pWave increasing to the East
2010 (Lower energy year)	Portugal	25 to 29	pWave increasing to the North
	Ireland	35	pWave is very homogeneous North to South
	Scotland	37 and 30	the Hebrides and Orkney
	North Sea	4 to 8	pWave increasing to the East
2012 (Lower energy year)	Portugal	23 to 27	pWave increasing to the North
	Ireland	45 to 47	Similar from North to South
	Scotland	45 and 40	the Hebrides and Orkney
	North Sea	3.5 to 9	pWave increasing to the East

This project has received funding from the Europeans Union's Horizon 2020 research & innovation programme under grant agreement number 101036457.

3 Limitations of wave energy assessment with global models

Several global reanalysis or hindcasts available these days provide extensive spatial and temporal coverage. They represent a useful (and easy to access) source to draw an initial mapping of the wave resource, but there are some important limitations to consider when interpreting the results of an analysis based on these data sources (like the one performed in the present document).

The first, and probably most obvious limitation is the spatial resolution of global models, typically ranging from 0.5° to 0.25° (~0.3° in the case of the ERA5 wave product), which is equivalent to ~55 km to ~27 km. Thus, it could be generalized that the closest output from the models' gridded data is about 20 to 30 km offshore. In most cases this corresponds to deep water conditions, where wave propagation is not affected by interactions with the surrounding bathymetry.

In Figure 13 an example is given to visualize the closest position to the coast from which a global model provides wave data. In some regions where these models compute results for shallower depth conditions (e.g. North Sea), they normally do not properly resolve bathymetric features which can easily be translated to an over or under estimation of wave heights (Alday, et al., 2022) (Lavidas & Vengatesan, 2018)

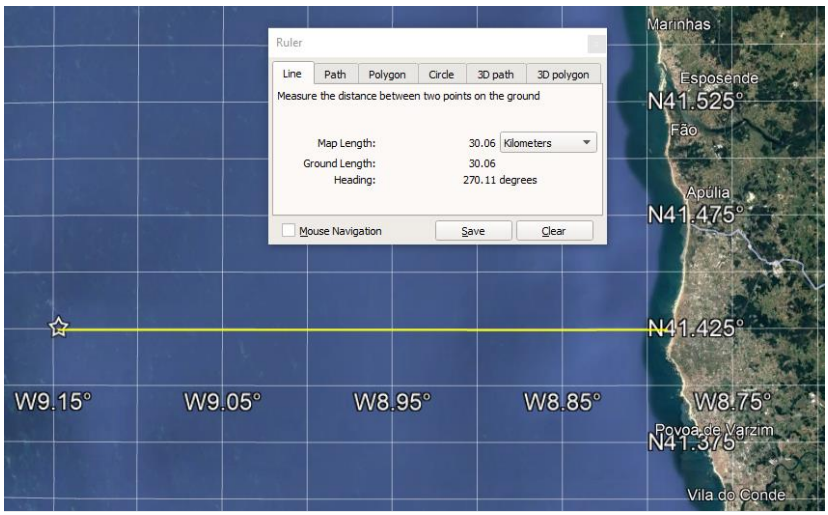

Figure 13. Representation of last grid node position with wave data offshore Aguçadoura, Portugal.

Map image taken from Google Earth. Star marks 30 km distance from the coast.

Another important element to take into account, and that has a direct impact on the models' output, is the different choices of forcing fields (Cavaleri & Bertolli, 1997), physical parameterizations and their adjustment to reduce model errors (Ardhuin, et al., 2010; Alday, et al., 2021). The latter point

This project has received funding from the Europeans Union's Horizon 2020 research & innovation programme under grant agreement number 101036457.

requires special attention, since the "tuning" of models could be done to improve overall performance, climatology estimates, or to improve results within a specific region. The latter point is probably the most important to generate adequate boundary conditions for (nesting) high-resolution models, with suitable shallow water models (e.g.; Simulating Waves Nearshore-SWAN) (Lavidas, et al., 2019).

Finally, an aspect sometimes overlooked, is the access to time series of wave parameters at locations representative of the sites of interest. This is especially important to assess the accuracy of the modelled data against in situ measurements which helps to estimate uncertainties (e.g.; random errors, bias, etc.; see Figure 14). While at deeper water altimeter data can be used, moving closer to the coastlines use of in-situ measurements is advised, as altimeter data cannot resolve and have limited performance (Cavaleri, et al., 2019).

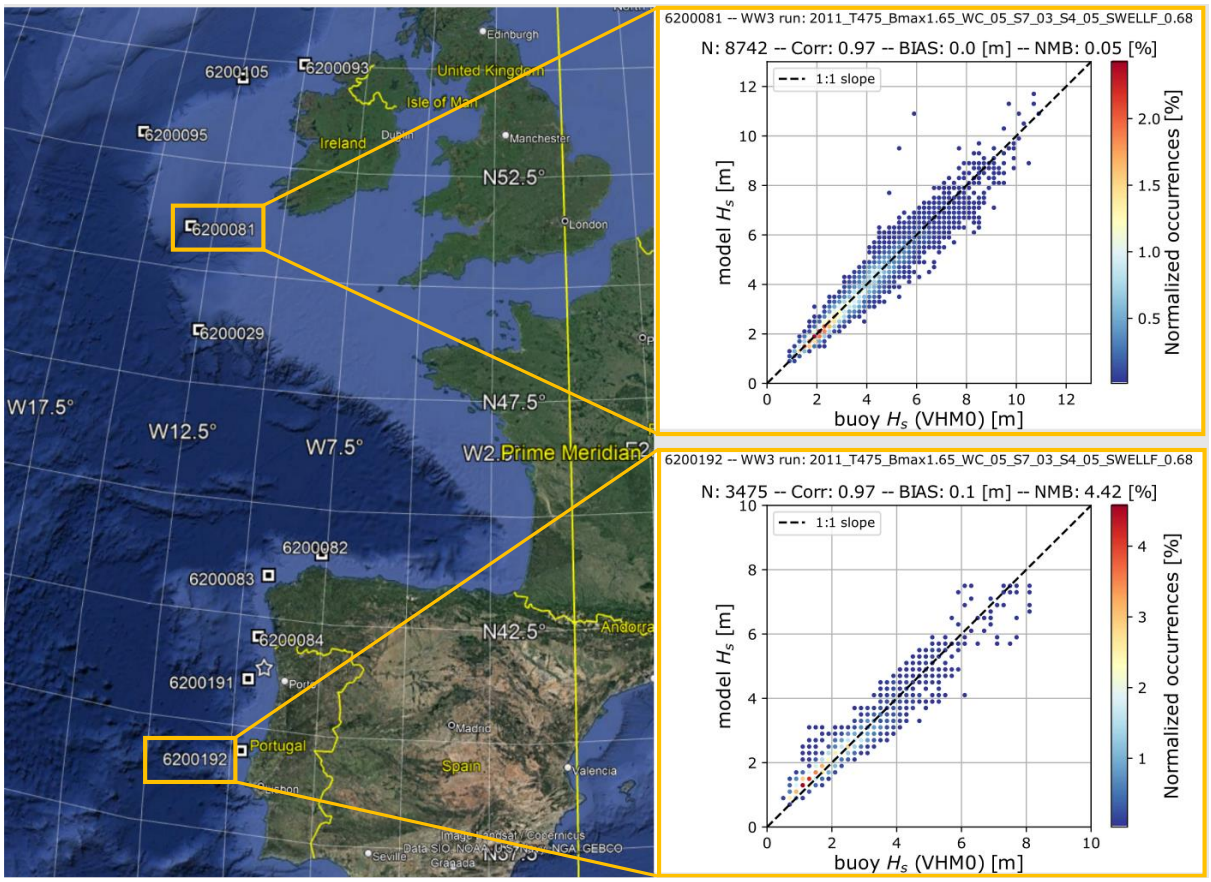

Figure 14. Example of the TU Delft North Atlantic model output at deep waters buoys location. Analyzed year : 2011.

Example of performance analysis for model adjustments. N is the total amount of analyzed data (only model-buoy time-matched pairs) in 1 year simulation. H_s bin size is 0.2 m. Map image taken from Google Earth.

This project has received funding from the Europeans Union's Horizon 2020 research & innovation programme under grant agreement number 101036457.

4 Wave database construction

To fulfil the requirements of the next steps of the project, in order to perform a more accurate wave resource assessment, a specially designed model implementation is currently ongoing. The modelling pipeline includes the following:

i. A "basin scale" regular grid of the North Atlantic.

ii. A high-resolution European regional (nested) model which takes spectral boundary conditions from the North Atlantic grid.

iii. A set of custom nearshore models for specific locations of interest within the scopes of the EU-SCORES project defined with the consortium partners.

iv. The North Atlantic grid and the European regional model are implemented using the WAVEWATCH III[2] spectral model (The WAVEWATCH III® Development Group, 2019).

v. The SWAN model (Booij, et al., 1997), developed in TU Delft, will be used for nearshore simulations, as it can allow more detailed solving of nearshore processes affecting wave propagation.

4.1 North Atlantic model implementation

The North Atlantic grid is considered fundamental for the generation of proper boundary conditions, and thus improve the sea states estimation in subsequent nested models for shallower depths.

Details of the model implementation are provided in the following subsections.

4.1.1 Forcing fields

The model setup includes the following forcing field:

i. ECMWF ERA5 reanalysis surface winds (Hersbach, et al., 2020).

ii. Surfaces current fields from CMEMS-Globcurrent (Global Ocean Multi Observation Product, MULTIOBS_GLO_PHY_REP_015_004) (Rio, et al., 2014; Mulet, et al., 2021). This correspond to combined geostrophic and Stokes drift driven currents.

[2] From here on WW3

This project has received funding from the Europeans Union's Horizon 2020 research & innovation programme under grant agreement number 101036457.

iii. Artic ice daily concentration from the Ifremer SSMI product (Girard-Ardhuin & Ezraty, 2012). A maximum thickness of 1 m at the ice edge is assumed.

4.1.2 Discretization and parameterizations

The North Atlantic basin model has a regular spatial resolution of 0.25°. It extends from longitude -99.5° to 49.75°, and latitudes 0.25° to 80°. The wave spectrum is discretized in 36 directions, equivalent to a directional resolution of 10°, and 36 exponentially spaced frequencies from 0.034 to 0.95 Hz, with a 1.1 increment factor.

The WW3 ST4 source term package is employed to account for wind-wave growth, deep waters wave breaking and swell dissipation effects (Ardhuin, et al., 2010).

4.1.3 Calibration (model adjustments) and validation (on-going)

Adjustments of the physical parameterizations are ongoing. This process is divided in 2 phases: Model performance analysis with altimetry data (e.g. Figure 15), and localized verification with wave parameters from buoys located in deep to intermediate waters (e.g., Figure 14).

Altimeter data are taken from the ESA Sea State Climate Change Initiative V3 product (Piollé, et al., 2022). Buoy data from the CMEMS in Situ TAC platform is used for calibration/validation at specific locations.

This project has received funding from the Europeans Union's Horizon 2020 research & innovation programme under grant agreement number 101036457.

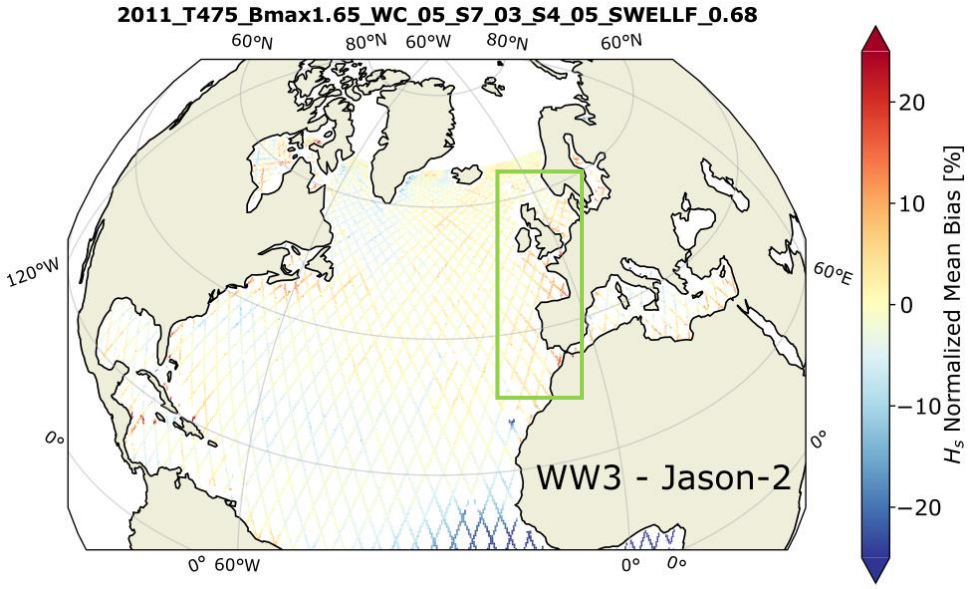

Figure 15. Example of the TU Delft North Atlantic model performance analysis using altimeter data (Jason-2).

H_s Normalized Mean Bias is computed with 1 year test simulation (2011 in this case). Green rectangle illustrates coverage of the high resolution regional model to be implemented.

4.2 Europe regional model generalities

After the North Atlantic grid adjustments of physical parameterizations and subsequent validation, boundary conditions will be generated to nest the European regional high-resolution model. Two options have been considered with respect to the resolution optimization: the implementation of an unstructured mesh, or a series of progressive nested models with a 2-way nesting approach. It should be noted that the regional model does not include the Mediterranean Sea. At this stage, only the domain of the European model has been defined (Figure 16). It will cover from longitude -20° to 12.5° and from latitude 31.5° to 63.5° (Figure 15).

A minimum resolution of ~15 km is estimated at the deep-water boundaries with progressive increase of resolution up to ~500-400 m along the coast. Physical parameterizations for wind-wave growth, wave breaking and swell dissipation, and spectral resolution (directions and frequencies) will be the same as in the North Atlantic grid.

This project has received funding from the Europeans Union's Horizon 2020 research & innovation programme under grant agreement number 101036457.

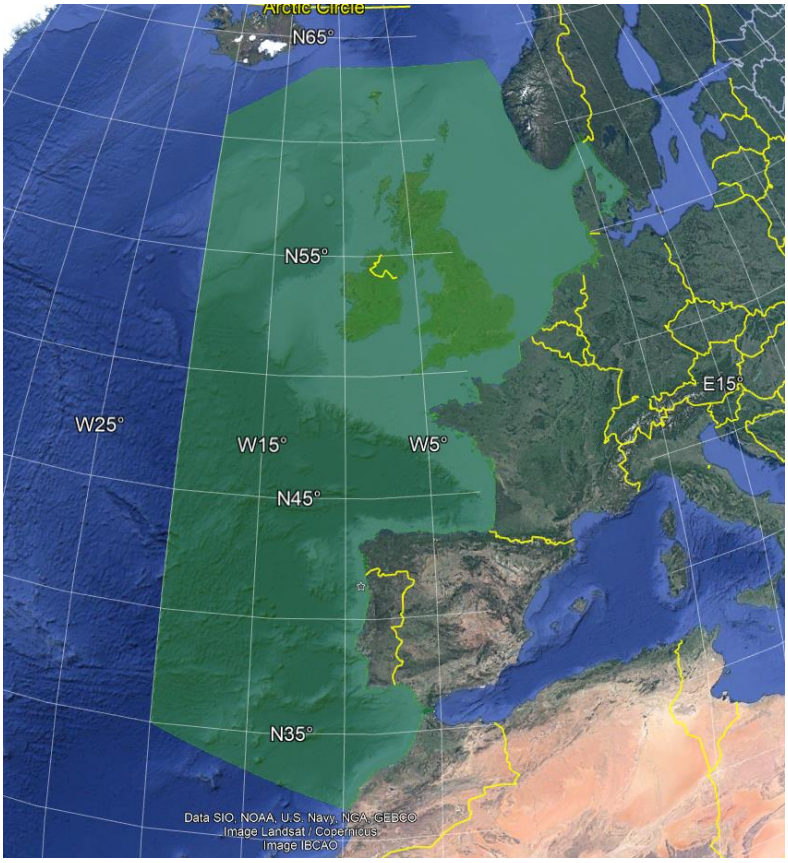

Figure 16. European regional model domain layout.
Map image taken from Google Earth.

This project has received funding from the Europeans Union's Horizon 2020 research & innovation programme under grant agreement number 101036457.

5 Wind resource coarse assessment

A preliminary study of wind speed and wind power density over Europe is conducted using the ERA5 reanalysis data (Hersbach, et al., 2020). As specified before, the data is having a spatial resolution of 0.3° at a temporal frequency of 1 hour. The data is collected for 30 years during 1990 to 2020, over the entire Europe covering the region between 30° N to 69.9° N, and 19° W to 41.9° E. The ERA5 data consists of a vast number of variables, out of which U_{100} (U component wind speed at 100 m height) and V_{100} (V component wind speed at 100 m height) are the variables considered for the coarse maps assessment. Using these variables, wind speed and wind power density are evaluated following Equation 5 and Equation 6.

Equation 5 $$\boldsymbol{wind\ speed(ws) = \sqrt{U_{100}^2 + V_{100}^2}}$$

In equation 6, U_{100} is the U wind speed component at 100 m height and V_{100} is the V wind speed component at 100 m height.

Equation 6 $$\textbf{wind power density} = \frac{1}{2}\rho(\textbf{wind speed})^3$$

In Equation 6, the air density is taken as 1.2258 kg/m^3.

In subsection 5.1, the wind speed climate characteristics are evaluated at different time scales using various evaluation metrices. Then, a similar methodology is applied for wind power density coarse assessment and presented in subsection 5.2.

5.1 Wind climate characterization

Before even analyzing the wind climate characteristics, an understanding of the distribution of wind speed is of paramount importance. In doing so, the wind speed at four random locations is binned at 1 m/s intervals and their histograms are visualized. The four locations considered for the wind speed distribution analysis are given in Table 2, which are location 1: Gulf of Lion, location 2: coast of Belgium, location 3: coast of Ireland, and location 4: Bay of Biscay.

Table 2: Details of the four locations considered for wind distribution analysis.

S No.	Location	North	East
1	Gulf of Lion	43.2	3.5
2	Coast of Belgium	51.6	2.6
3	Coast of Ireland	52.8	-10.3
4	Bay of Biscay	45.3	1.4

Over these four locations, histograms of the wind speed collected during 1990 to 2020 at 1 hour interval are presented in Figure 17. These histograms clearly indicate the bell shaped

This project has received funding from the Europeans Union's Horizon 2020 research & innovation programme under grant agreement number 101036457.

(Normal) distribution skewed towards right. Wind speeds between 3 to 6 m/s are more frequent over the Gulf of Lion and the Bay of Biscay, whereas 8 to 11 m/s are more frequent over the Coast of Belgium and Ireland. In cases with skewed data, application of the Weibull distribution is more suitable which is characterized by its slope and scale parameters, as follows.

Equation 7

$$\mathbf{f(v) = \frac{k}{c}\left(\frac{v}{c}\right)^{k-1} exp\left[-\left(\frac{v}{c}\right)^{k}\right]}$$

Where, k is the slope parameter and c is the scale parameter. Slope parameter higher than 1 indicates a bell-shaped distribution, equals to 1 implies the exponential distribution, and less than 1 indicates an exponent distribution.

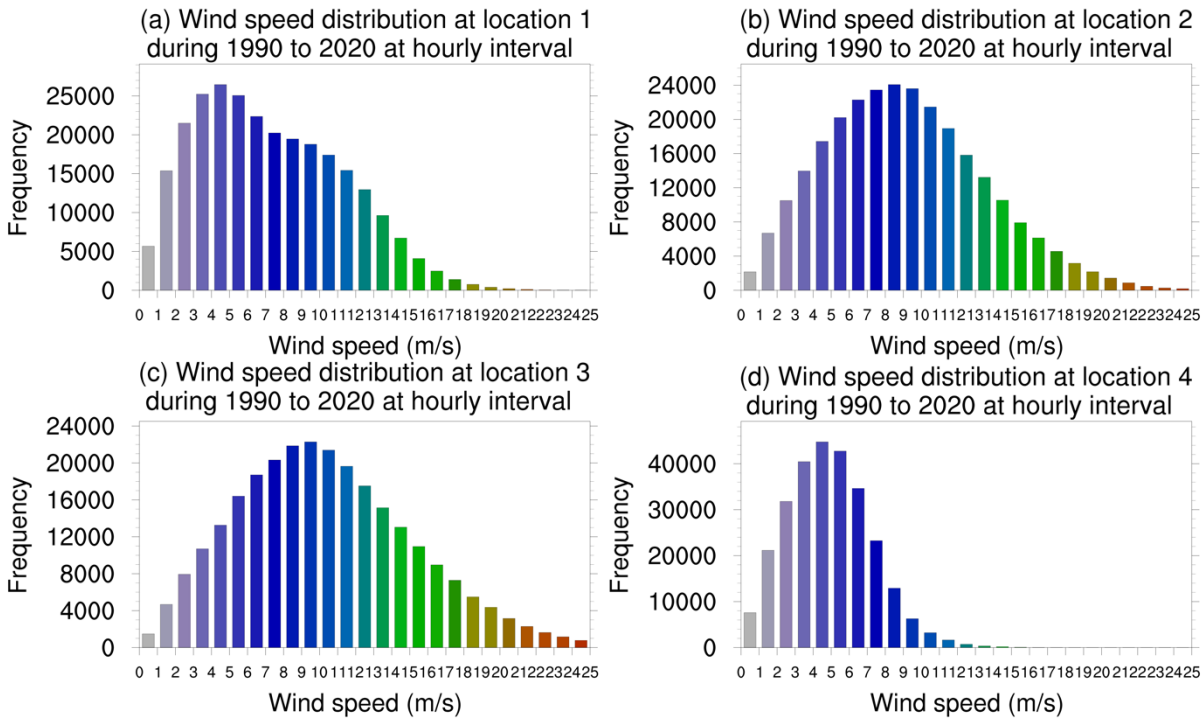

Figure 17: Histograms of wind speed at locations (a) Gulf of Lion, (b) coast of Belgium, (c) coast of Ireland, and (d) Bay of Biscay.

The climate characteristics of wind speed are evaluated using mean (Equation 1), covariance (CoV) (Equation 3), and Weibull slope parameter (k) (Equation 7), for different time scales, such as yearly, seasonal, and overall. The mean parameter resonates the expectation of a variable, whereas the CoV and k resonate the variability of that expectation. The CoV and the slope parameters directly imply the variability in the data, such that a high CoV or a low slope parameter indicates higher variability.

Figure 18 shows the overall mean, Weibull distribution slope parameter, and coefficient of variance, of wind speed during

This project has received funding from the Europeans Union's Horizon 2020 research & innovation programme under grant agreement number 101036457.

1990 to 2020. The North Sea receives fairly 10 m/s winds with a CoV of 0.4 and k of 2.2, which indicate that the wind speed over this location varies very little to the mean value. The west coast of Ireland receives 12 m/s wind speed with low variability, whereas the coast of Belgium and Germany receive 10 m/s mean wind speed with a similar variability. The Mediterranean Sea receives way less wind speed at 6 m/s, with Gulf of Lion being an exceptional case, receiving winds at 10 m/s but with high variability. North coast of Portugal and Spain receive 8 m/s but the variability is really high compared to other locations.

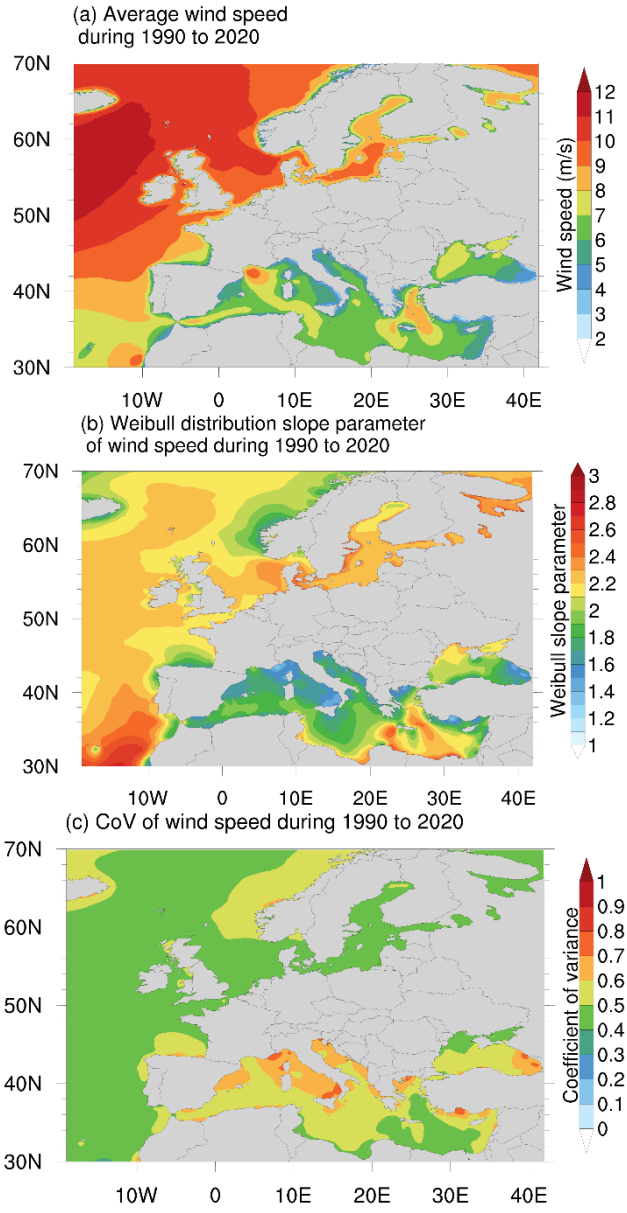

Figure 18: (a) Mean, (b) Weibull distribution slope parameter, and (c) coefficient of variation of hourly wind speed during 1990 to 2020.

This project has received funding from the Europeans Union's Horizon 2020 research & innovation programme under grant agreement number 101036457.

In addition, the peak or low wind years are identified based on the percentage deviation of annual mean wind speed to that of the overall 30 years mean, as follows:

Equation 8

$$\mathbf{DEV} = \frac{\textbf{Yearly mean} - \textbf{30 years mean}}{\textbf{30 years mean}} \times \mathbf{100}$$

Figure 18 to Figure 20 show the yearly mean wind speed deviation for years 1990 to 2020. From these figures, it is evident that the mean wind speed during 1990, 2015, 2020 is higher than the overall mean by 12% to 16%, over the majority of the area. These years are considered as peak wind years. In contrast, the mean wind speed during 2001, 2003, and 2010 is lower than the overall mean by 12% to 20%, over the majority of the area. These years are considered as the low wind years.

This project has received funding from the Europeans Union's Horizon 2020 research & innovation programme under grant agreement number 101036457.

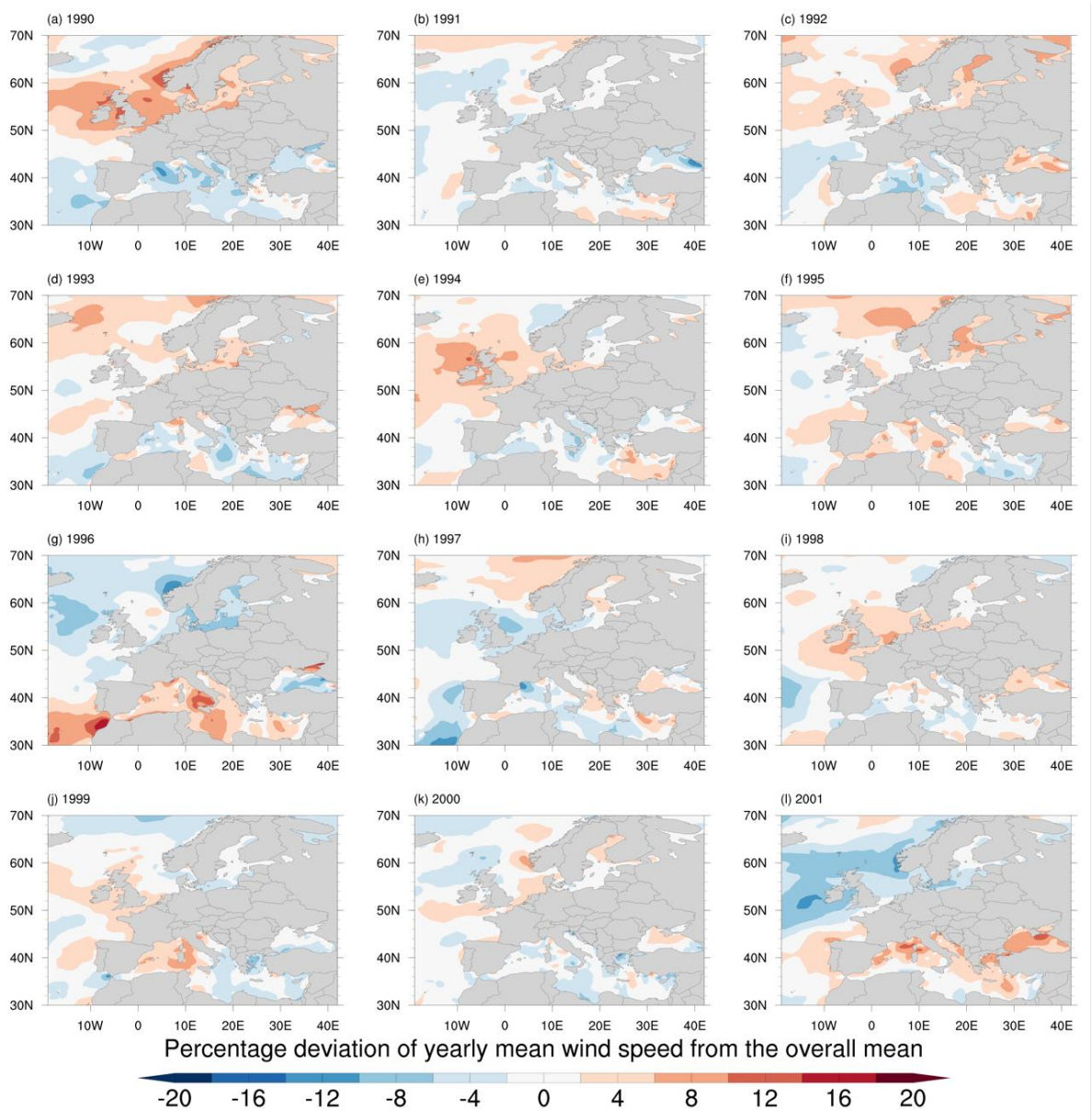

Figure 19: Percentage deviation of yearly mean wind speed from 30 years mean wind speed.

This project has received funding from the Europeans Union's Horizon 2020 research & innovation programme under grant agreement number 101036457.

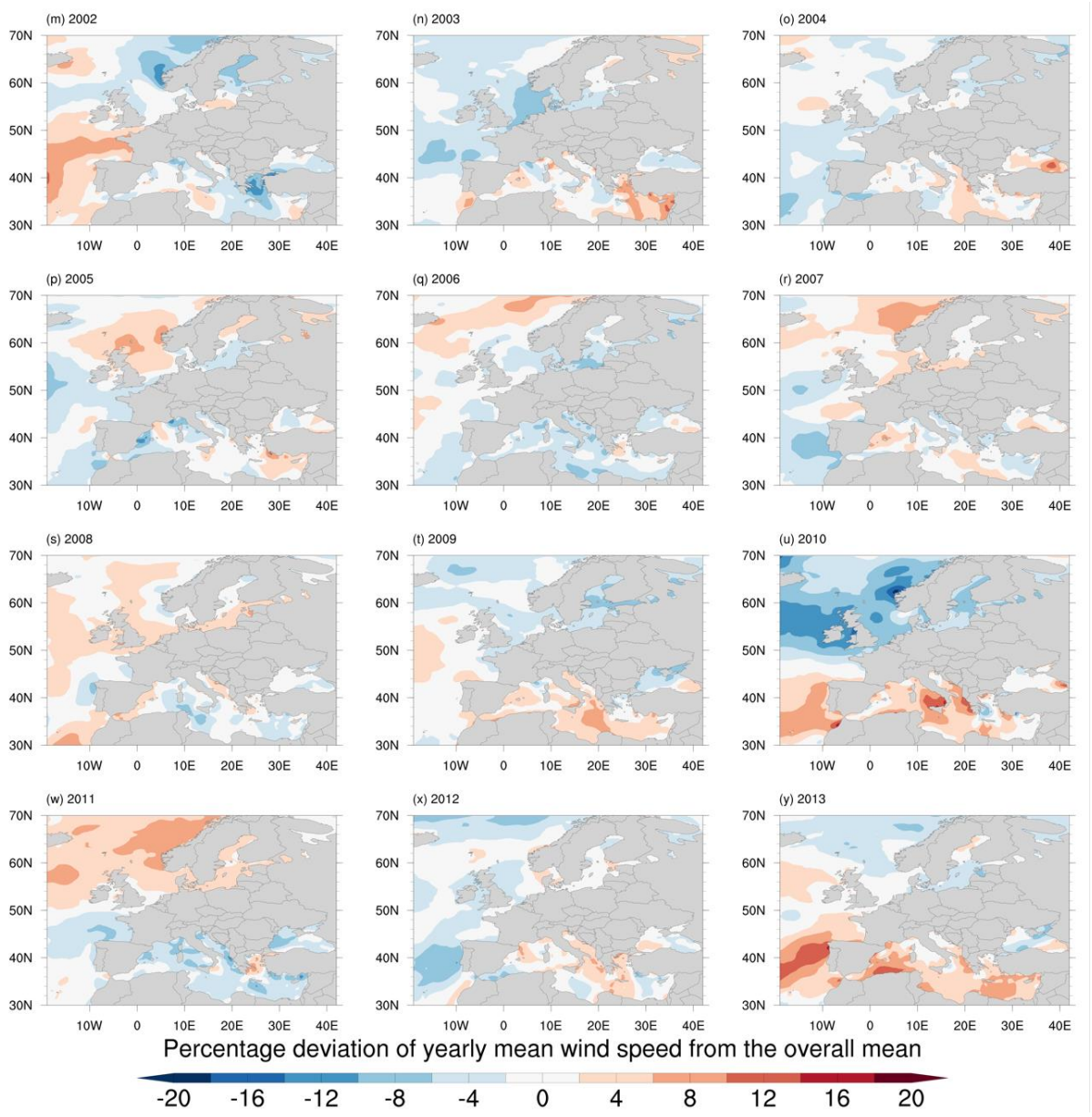

Figure 20: Percentage deviation of yearly mean wind speed from 30 years mean wind speed (Continuation)

This project has received funding from the Europeans Union's Horizon 2020 research & innovation programme under grant agreement number 101036457.

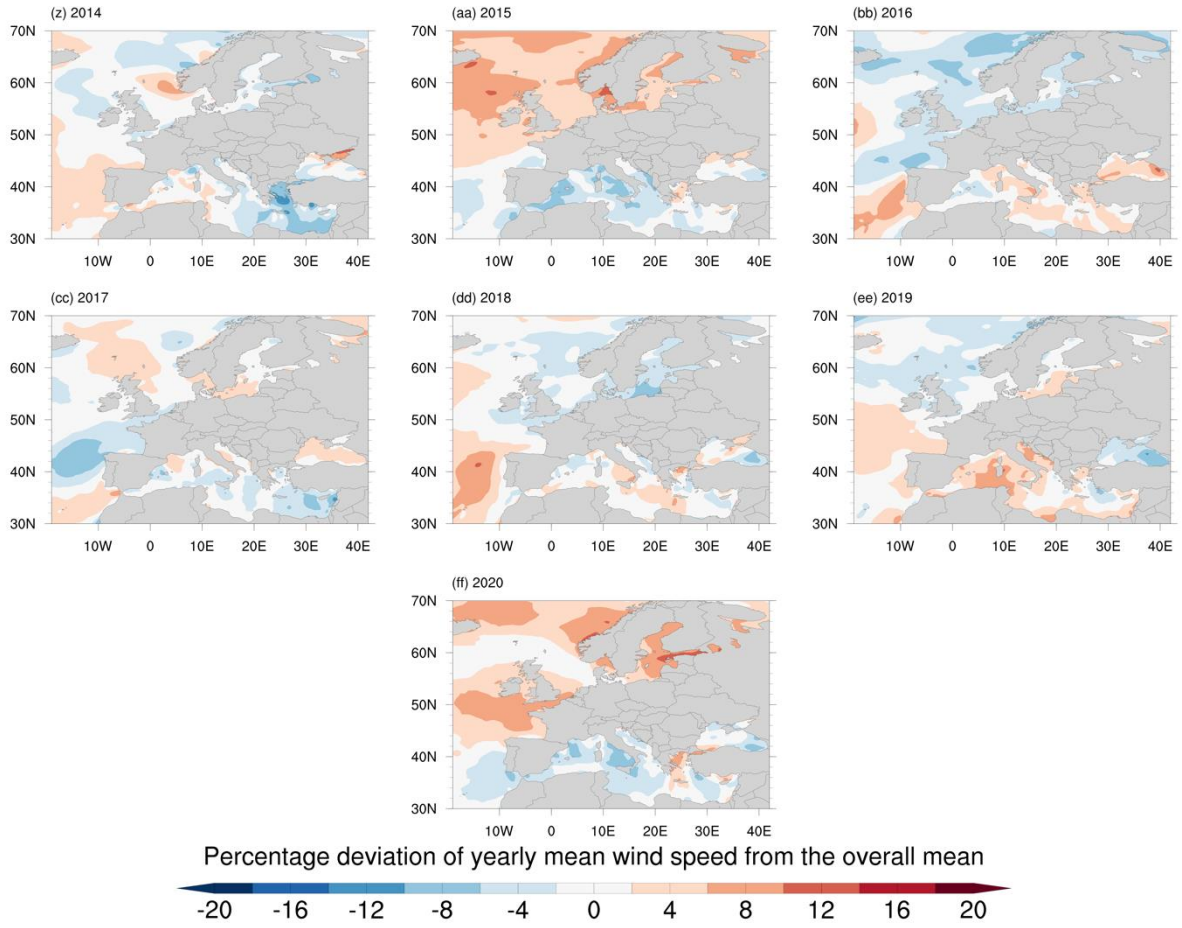

Figure 21: Percentage deviation of yearly mean wind speed from 30 years mean wind speed (Continuation)

Figure 22 and Figure 23 illustrate the wind characteristics of peak and low wind years. During the peak wind years, the North Sea receives 11 m/s wind speed with low variability and the coast of Ireland receive 12 m/s wind speed with a similar variability. During the low wind years, the same areas receive at least an order of 1 m/s lower winds. In contrast, the Mediterranean Sea receive higher winds during low wind years and lower winds during peak wind years. Apart from the mean wind speed, the variability characteristics are fairly similar during the peak and low wind years if we look at it as a whole. To understand the characteristics in detail, further analysis is needed by selecting some specific locations.

This project has received funding from the Europeans Union's Horizon 2020 research & innovation programme under grant agreement number 101036457.

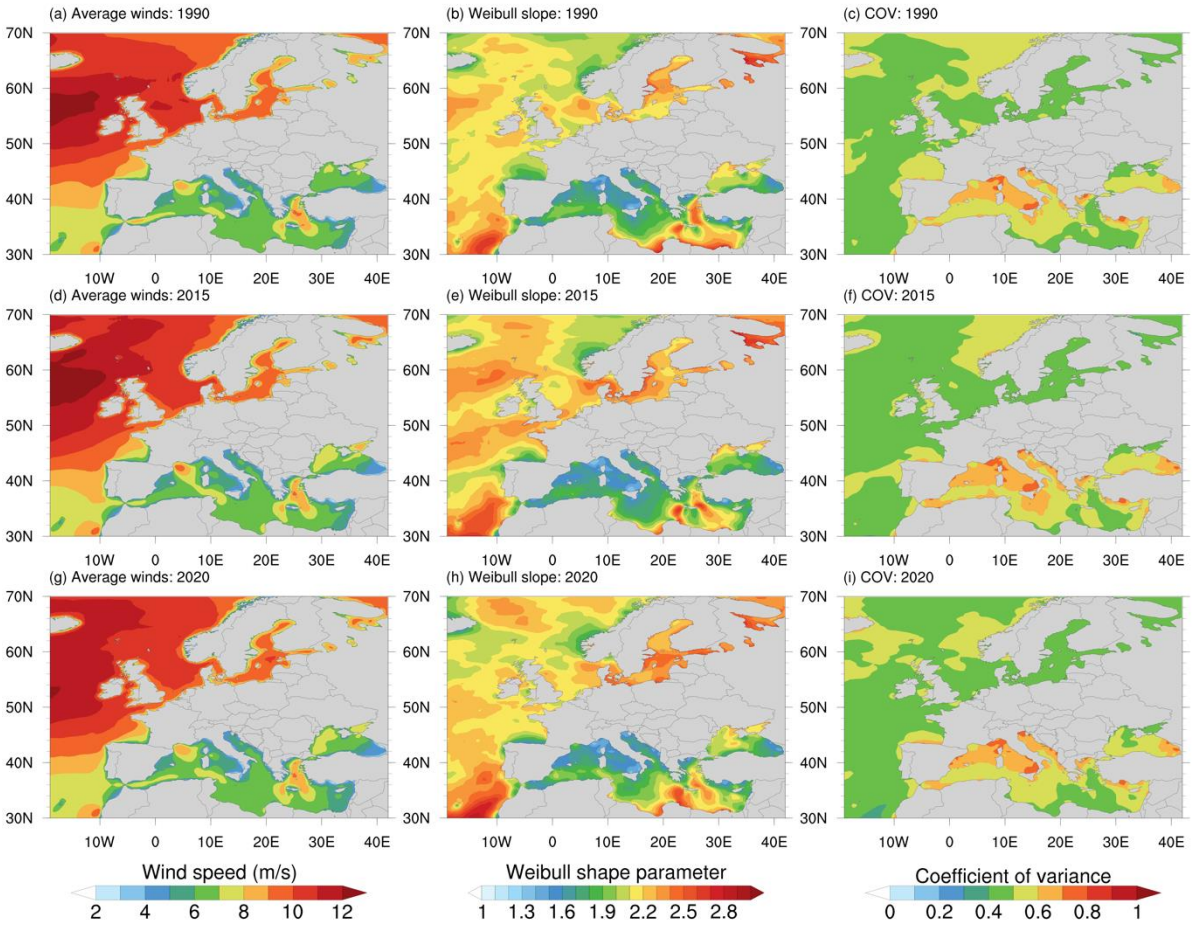

Figure 22: (a-g) Mean, (b-h) Weibull distribution slope parameter, and (c-i) coefficient of variation of hourly wind speed during peak wind years (a-c) 1990, (d-f) 2015, and (g-i) 2020.

This project has received funding from the Europeans Union's Horizon 2020 research & innovation programme under grant agreement number 101036457.

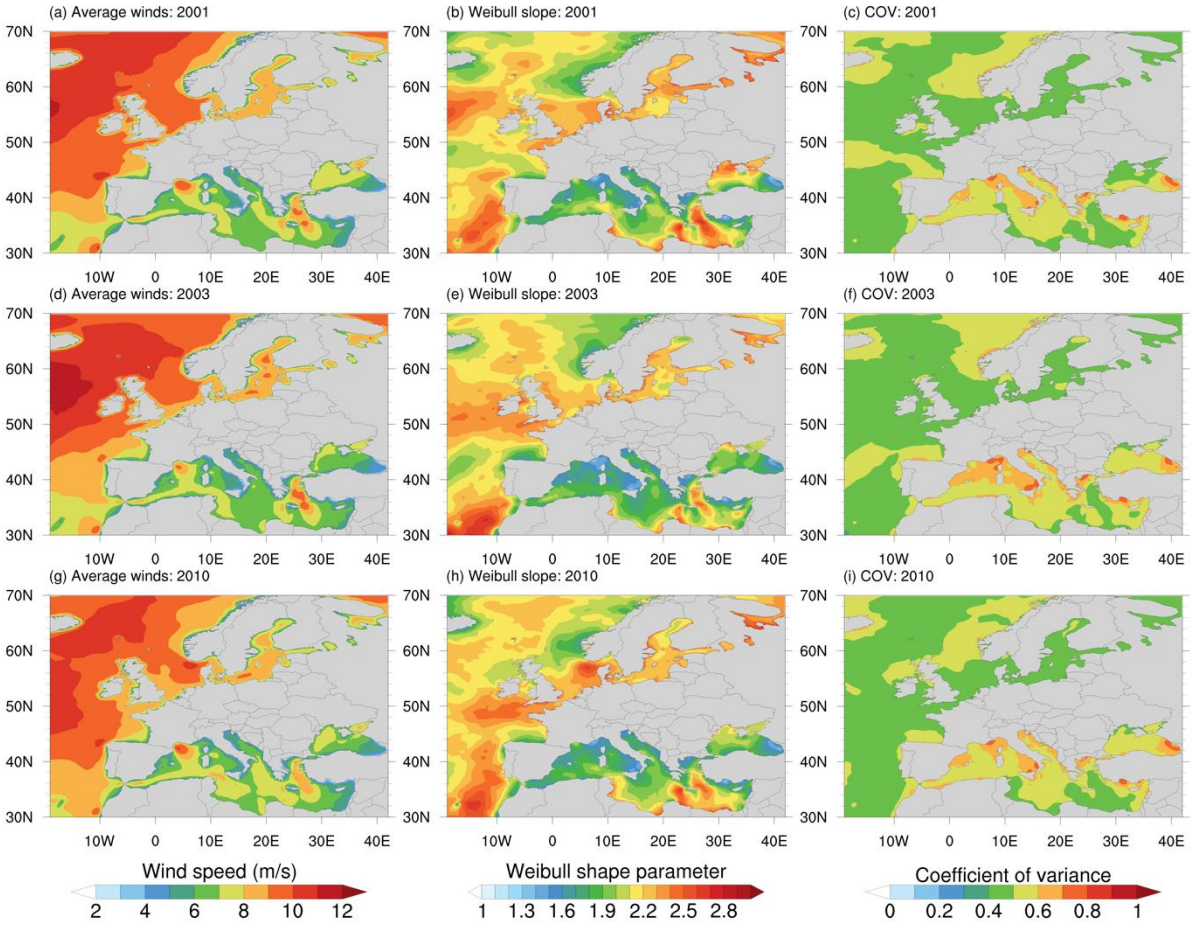

Figure 23: (a-g) Mean, (b-h) Weibull distribution slope parameter, and (c-i) coefficient of variation of hourly wind speed during low wind years (a-c) 2001, (d-f) 2003, and (g-i) 2010.

Finally, the wind statistics are analysed on a seasonal time scale to understand the influence of different seasons on wind speeds and are presented in Figure 24.

From the figure, it is evident that the winds are maximum during winter and minimum during summer. Except for summer, the winds over the North Sea and Atlantic Ocean reach 10 m/s during the remaining three seasons. The winds during autumn and winter are more or less of similar intensity over the North Sea, however, the variability is high during winter compared to the autumn. This suggest that more gusty winds prevail during winter compared to any other season. One peculiar thing to note is the higher winds during summer compared to winter and autumn over the coast of Portugal, which could be attributed to the strong winds from tropics towards the subtropics.

This project has received funding from the Europeans Union's Horizon 2020 research & innovation programme under grant agreement number 101036457.

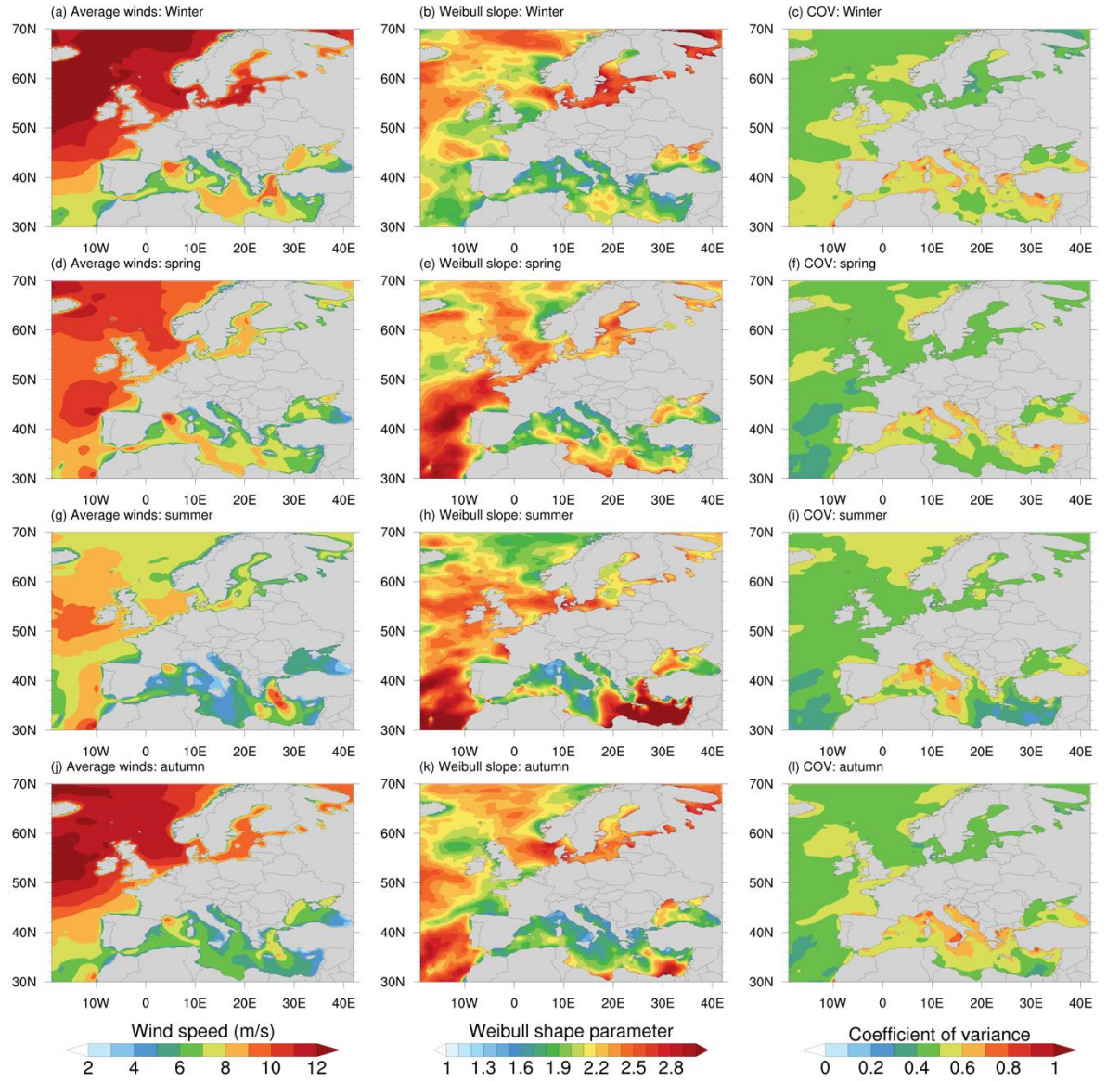

Figure 24: (a-j) Mean, (b-k) Weibull distribution slope parameter, and (c-l) coefficient of variation of hourly wind speed during seasons (a-c) winter, (d-f) spring, (g-i) summer, and (j-l) autumn.

This project has received funding from the Europeans Union's Horizon 2020 research & innovation programme under grant agreement number 101036457.

5.2 Wind power assessment

The wind power density is a derived quantity from *U* and *V* components of wind speed and is calculated using Equation 6. The wind power density at the four locations mentioned in Table 2 are binned at 50 W/m^2 intervals and their histograms are visualized in Figure 25. The wind power density follows an exponent distribution, rather than a normal distribution. One point to note is the distribution did not change even after taking the bin size as 10 W/m^2(not shown here), indicating the wind power density following an exponential distribution.

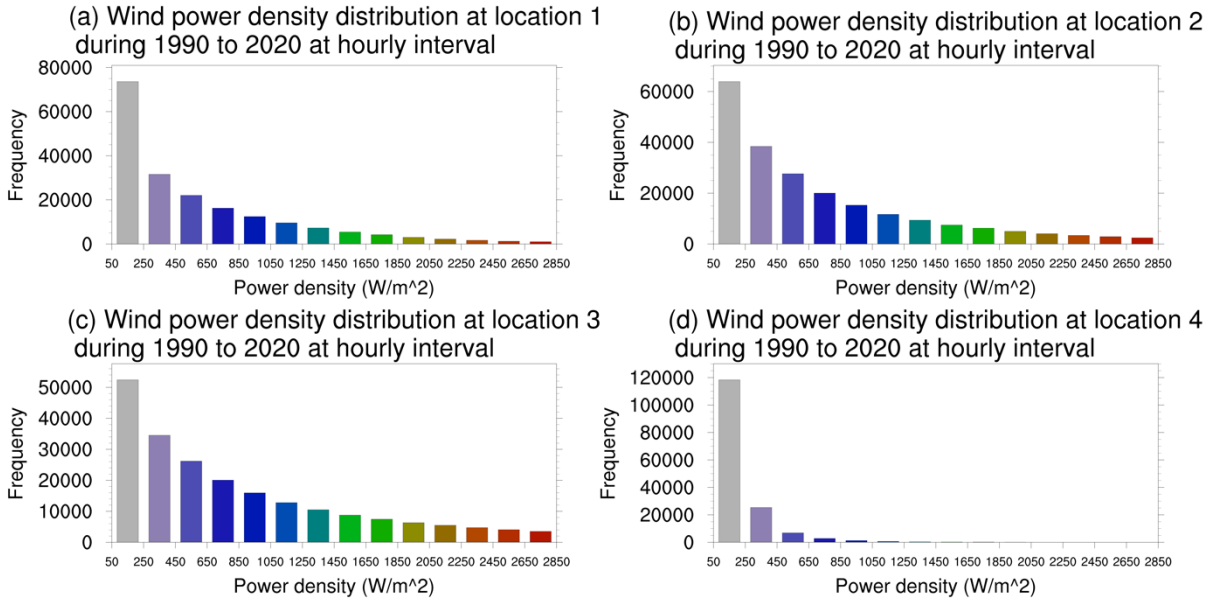

Figure 25: Histograms of wind power density at locations (a) Gulf of Lion, (b) coast of Belgium, (c) coast of Ireland, and (d) Bay of Biscay.

Figure 26 shows the overall mean, Weibull distribution slope parameter, and coefficient of variance, of wind power density during 1990 to 2020. From the figure, the North Sea and the coast of Belgium reaches 1100 W/m^2 power density, whereas the west coast of Ireland receives 1300 W/m^2, and the west coast of Portugal receives 600 W/m^2. Figure 26b indicates that the Weibull distribution slope parameter lies below 1, implying the power density follows an exponential distribution, confirms the results of Figure 25. The colour bar shown in Figure 26c indicates that the values of the coefficient of variance values remains above 1, whereas that of the wind speed are below 1, implying the variability in power density is higher compared to that of the wind speed.

Nevertheless, the Mediterranean Sea exhibits power densities below 300 W/m2 power density over many coastal areas with highest variability, implying the conditions are less favourable for offshore wind power production.

This project has received funding from the Europeans Union's Horizon 2020 research & innovation programme under grant agreement number 101036457.

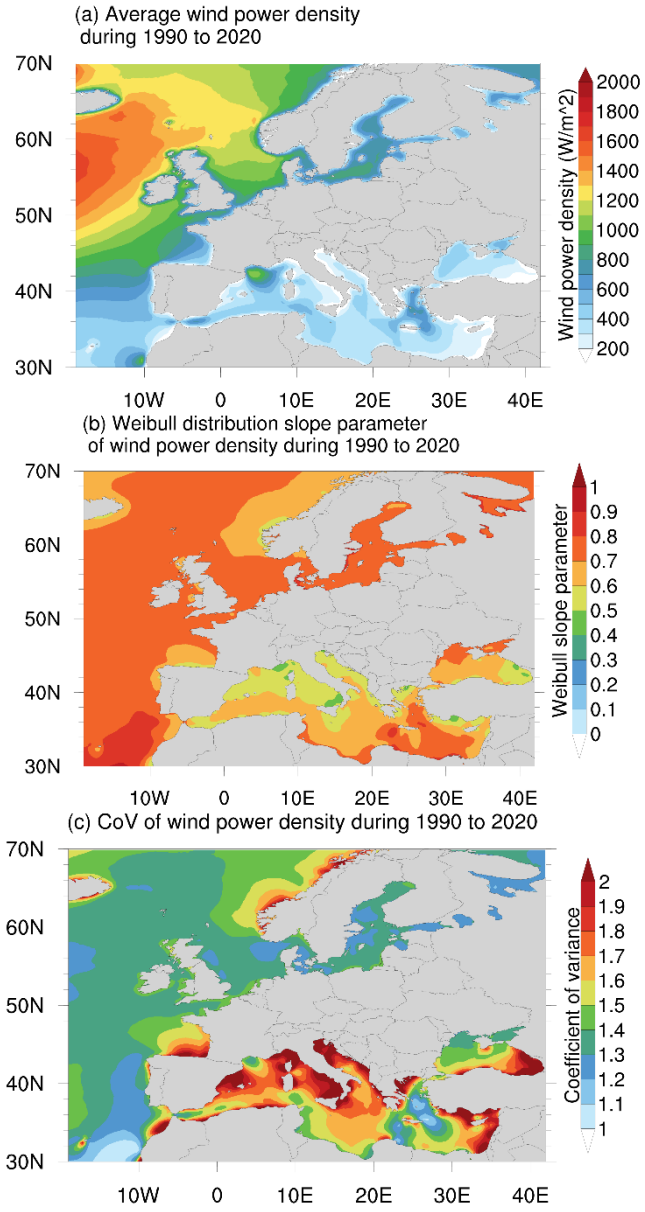

Figure 26: (a) Mean, (b) Weibull distribution slope parameter, and (c) coefficient of variation of hourly wind power density during 1990 to 2020.

In wind power production, the turbines' production characteristics are based on the respective power curves, which describe the expected generated power per wind speed bin. For example, five types of turbines and their power curves which are considered in the studies of (Li, et al., 2021) are presented in Figure 27. Based on the maximum power output above a rated wind speed the conversion efficiency depends on the choice of turbine and the site specific climate. Hence it is always advisable to examine the wind speed characteristics rather than power density itself for wind power production.

This project has received funding from the Europeans Union's Horizon 2020 research & innovation programme under grant agreement number 101036457.

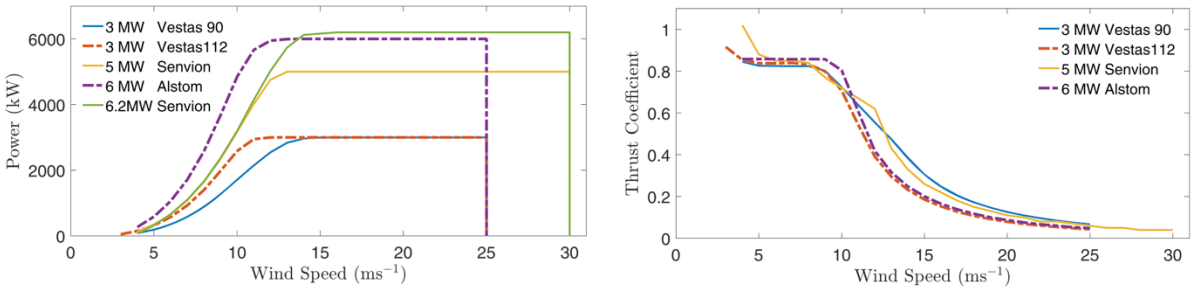

Figure 27: Power curves (left panel) and corresponding thrust curves of five turbines from the Belgian offshore wind farms. Figure taken from (Li, et al., 2021)

This project has received funding from the Europeans Union's Horizon 2020 research & innovation programme under grant agreement number 101036457.

6 Solar Energy coarse assessment

A preliminary study of solar energy coarse map assessment over Europe is conducted using the ERA5 reanalysis data. Out of the available variables, the air temperature at 2 meters above the ground (2 m temperature) and the solar radiation reaching the earth surface from all directions (surface solar radiation downward) are the two variables considered for the solar energy coarse assessment. The assessment is conducted for a period of 30 years from 1990 to 2020, at hourly, seasonal, yearly, and overall time scales.

6.1 Surface 2 m temperature characterization

The 2 m temperature at the four locations mentioned in Table 2 are binned at 2 °C intervals and their histograms are visualized in Figure 28. From the figure, it is evident that the 2 m temperature follows a bell-shaped distribution, with two peaks, indicating the influence of summer and winter temperature dominance.

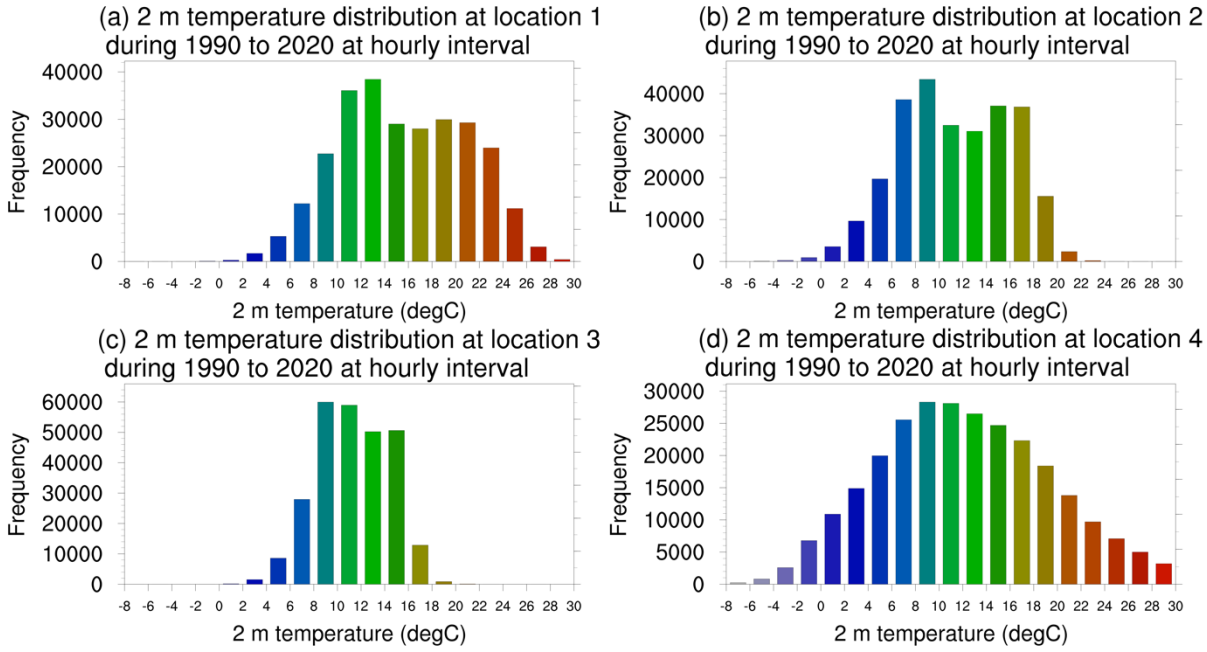

Figure 28: Histograms of 2 m temperature at locations (a) Gulf of Lion, (b) coast of Belgium, (c) coast of Ireland, and (d) Bay of Biscay.

Figure 29 shows the overall mean and coefficient of variance of 2 m temperature during 1990 to 2020. In theory, for a homogenous Earth, the surface temperature would be the same for two locations on the same latitude, which is due to the Earth rotation and availability of solar radiation. However, it is evident that the temperature over Europe is significantly higher

This project has received funding from the Europeans Union's Horizon 2020 research & innovation programme under grant agreement number 101036457.

compared to the Western Russia, which is within the same latitude, which is due to the Gulf Stream.

The Gulf Stream carries with it considerable heat when it flows out from the Gulf of Mexico and then north along the East Coast before departing U.S. waters at Cape Hatteras and heading northeast toward Europe. All along the way, it warms the overlying atmosphere. This provides western Europe with a milder climate as compared with other regions around the globe at the same latitude. The entire Europe is situated in the subtropical region, thus the maximum average temperature lies below 27 °C. The Mediterranean Sea, acting as a heat sink, provides the necessary heat to the surrounding countries, and keeping them sufficiently warm. The colorbar shown in Figure 29b indicates that the values of the coefficient of variance values lies between 0 and 0.1, implying the variability in 2 m temperature is very marginal. Nevertheless, the temperature variability over the Atlantic Ocean and Western Europe is very small compared to that of over the Eastern Europe.

This project has received funding from the Europeans Union's Horizon 2020 research & innovation programme under grant agreement number 101036457.

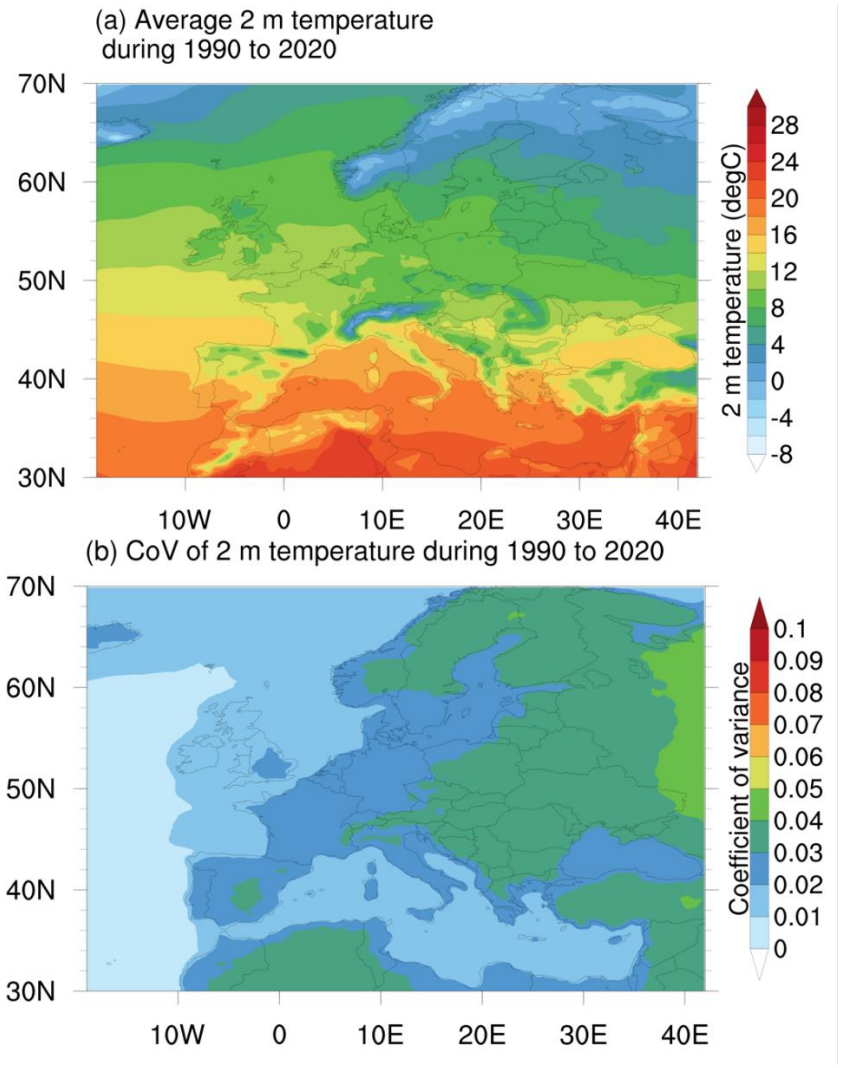

Figure 29: (a) Mean and (b) coefficient of variation of hourly 2 m temperature during 1990 to 2020.

Figure 30 shows the hourly average 2 m temperature averaged over 1990 to 2020, presented at every two hours. The surface temperature gradually increases as sun rises and reaches maximum at noon, and then gradually decreases as sun goes down. A peculiar observation is that during morning and evening, influence of the Gulf Stream dominates the surface temperature, whereas the sun radiation dominates during the noon. Throughout the day, temperature over western Europe is above 12 °C, and during noon it reaches approximately 17 °C.

This project has received funding from the Europeans Union's Horizon 2020 research & innovation programme under grant agreement number 101036457.

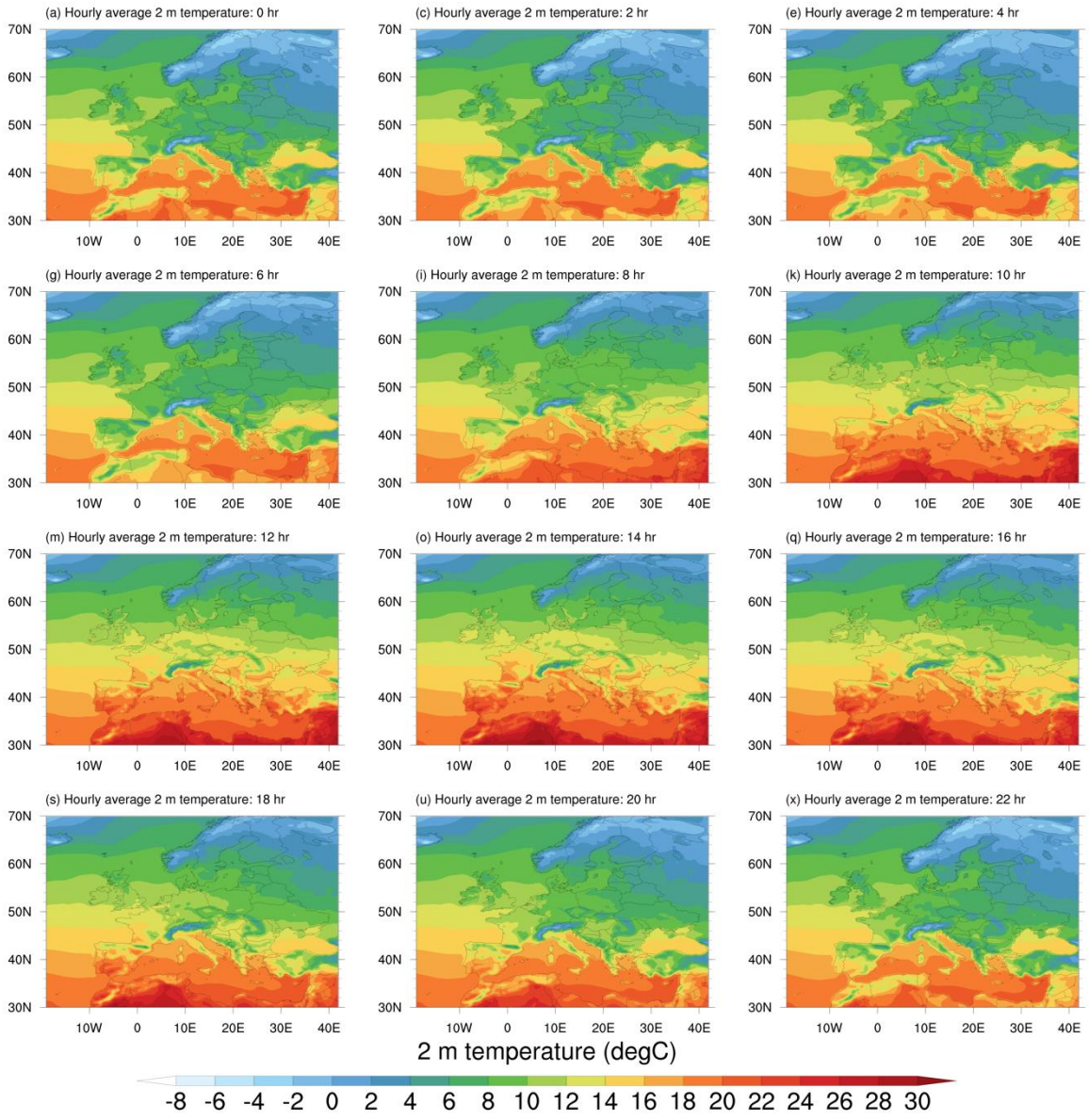

Figure 30: Mean hourly 2 m temperature averaged at every hour during1990 to 2020.

The 2 m temperature is analyzed at yearly time scale to identify the anomalies and their characteristics. The hot and cool years are identified based on the percentage deviation of annual mean 2 m temperature to that of the overall 30 years mean, as given in Equation 8.

Figure 31 until Figure 33 show the yearly mean 2 m temperature deviation for years 1990 to 2020. The color bar indicates the temperature deviation lie in between 2% of the overall mean. Though the percentage seems not a great deal, but the anomaly is clearly high. From these figures, it is evident that the annual mean 2 m temperature is lower than the overall mean during 1990 to 2000, indicating a continuous cold decade. In contrast,

This project has received funding from the Europeans Union's Horizon 2020 research & innovation programme under grant agreement number 101036457.

the annual mean 2 m temperature is way higher than the overall mean during 2010 to 2020, indicating a continuous hot decade.

A further examination of external factors, such as climatic phenomena, is needed to understand these cold and hot decades in detail. In addition, during 2014, 2018, and 2020, the annual means are higher than the overall mean by 0.6% to 1.3%, over the majority of the area. These years are considered as hot years. In contrast, the annual mean 2 m temperatures during 1991, 1993, and 1996 are lower than the overall mean by 0.6% to 1.2%, over majority of the area. These years are considered as the cold years.

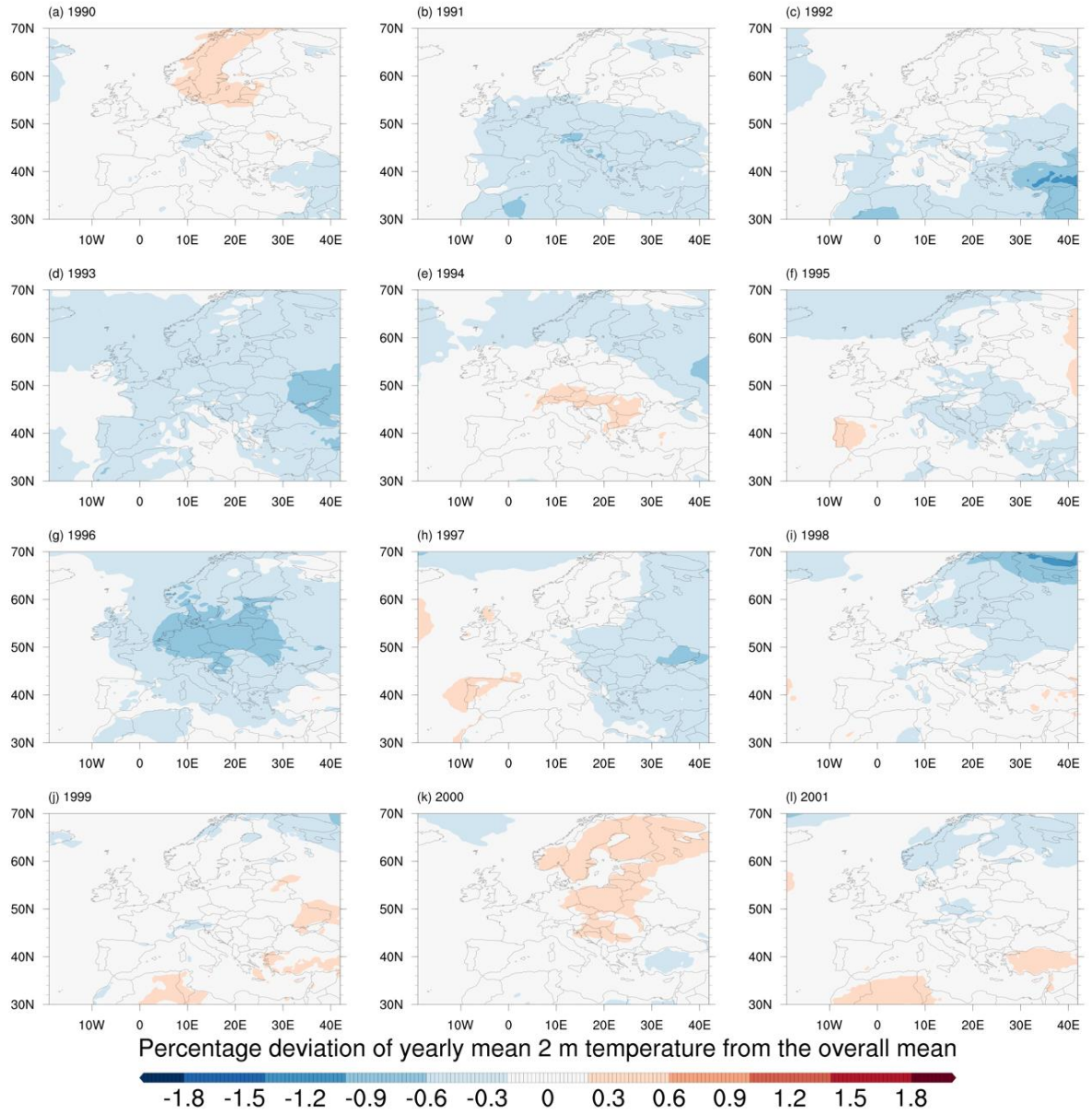

Figure 31: Percentage deviation of Yearly mean 2 m temperature from 30 years mean.

This project has received funding from the Europeans Union's Horizon 2020 research & innovation programme under grant agreement number 101036457.

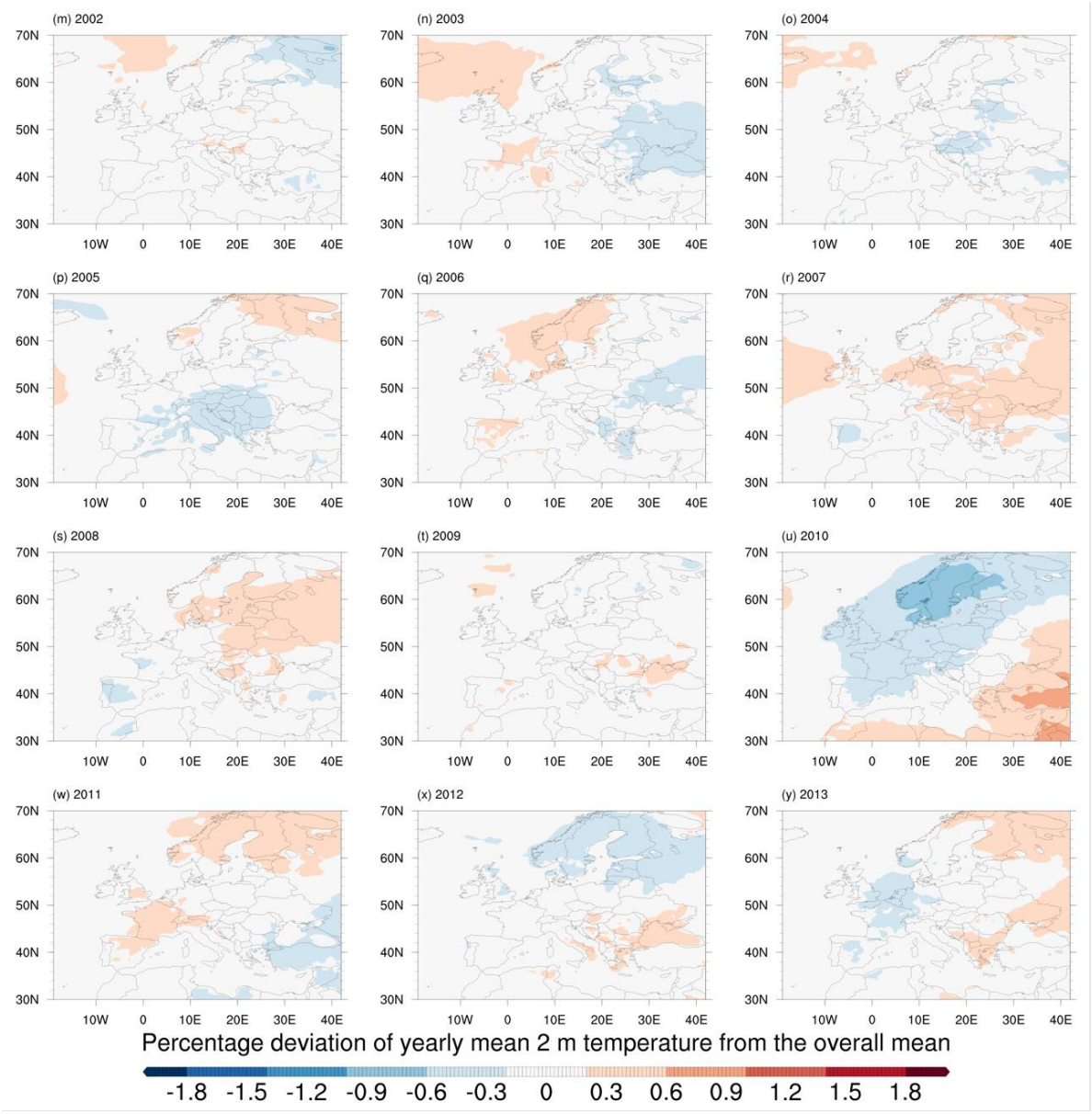

Figure 32: Percentage deviation of Yearly mean 2 m temperature from 30 years mean, (Continuation)

This project has received funding from the Europeans Union's Horizon 2020 research & innovation programme under grant agreement number 101036457.

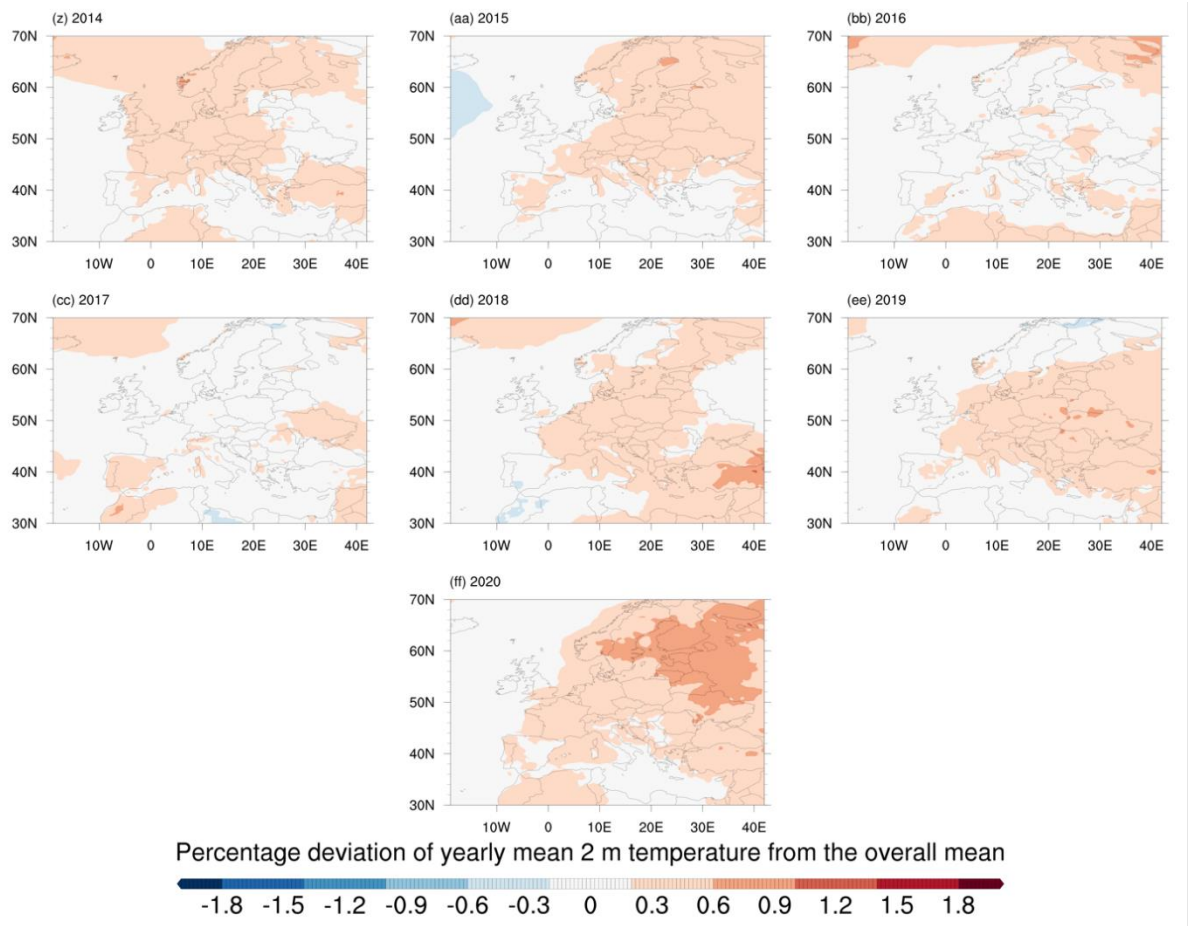

Figure 33: Percentage deviation of Yearly mean 2 m temperature from 30 years mean (Continuation)

Figure 34 and Figure 35 illustrate the 2 m temperature characteristics of hot and cold years. During the hot years, the 2 m temperature over the entire Europe from west to east as a stretch, reaches beyond 12 °C. In addition, many locations over the southern Europe also experience temperatures higher than 17 °C. In contrast, during the cold years, the temperatures over the eastern Europe are lower than the overall mean temperatures, and the southern Europe also experiences lower temperatures than the mean. In addition to this, the coefficient of variation during the hot years is lower than the overall, whereas during the cold years, it is higher.

This project has received funding from the Europeans Union's Horizon 2020 research & innovation programme under grant agreement number 101036457.

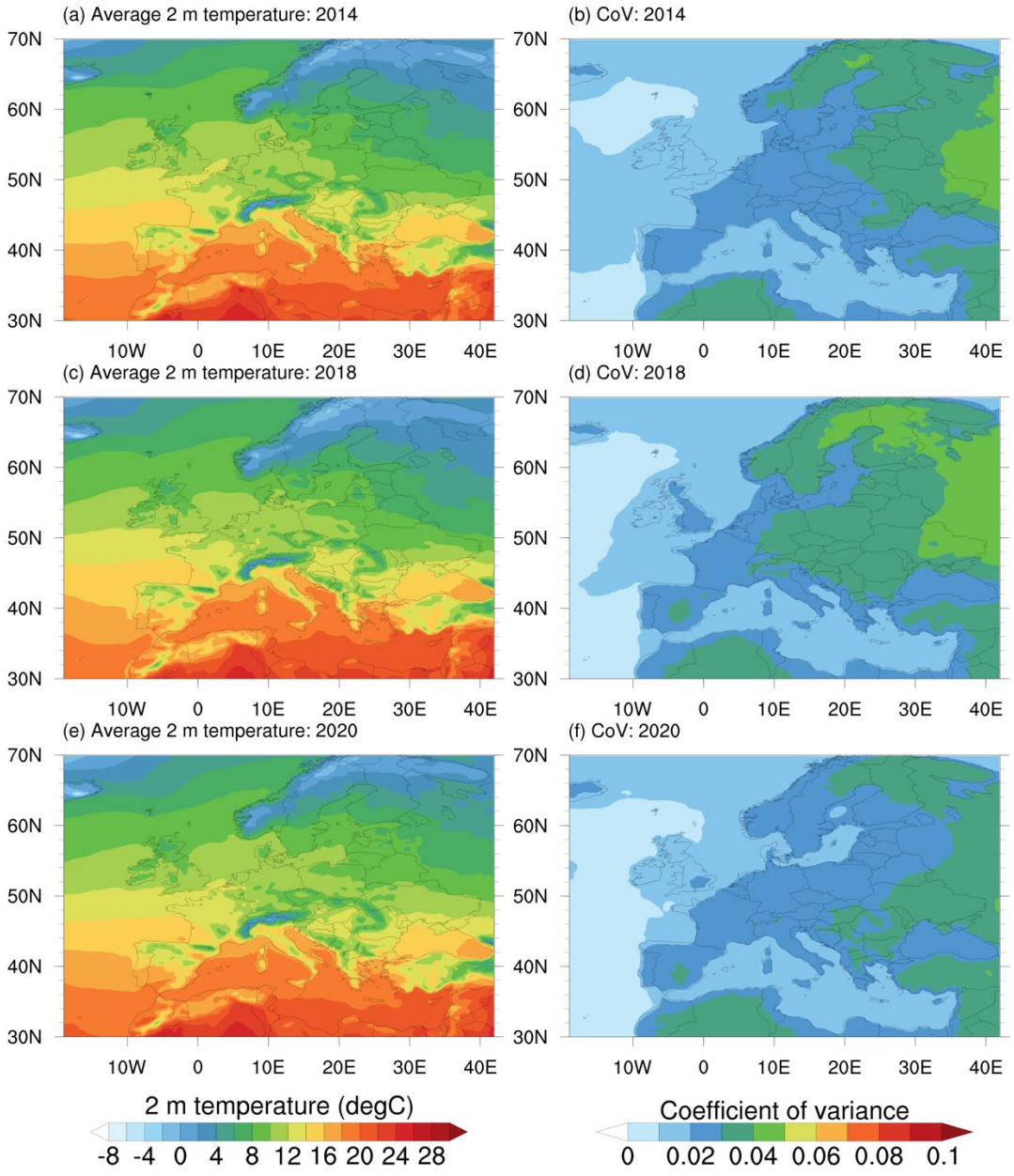

Figure 34: (a-e) Mean and (b-f) coefficient of variation of hourly 2 m temperature during hot years (a-b) 2014, (c-d) 2018, and (e-f) 2020.

This project has received funding from the Europeans Union's Horizon 2020 research & innovation programme under grant agreement number 101036457.

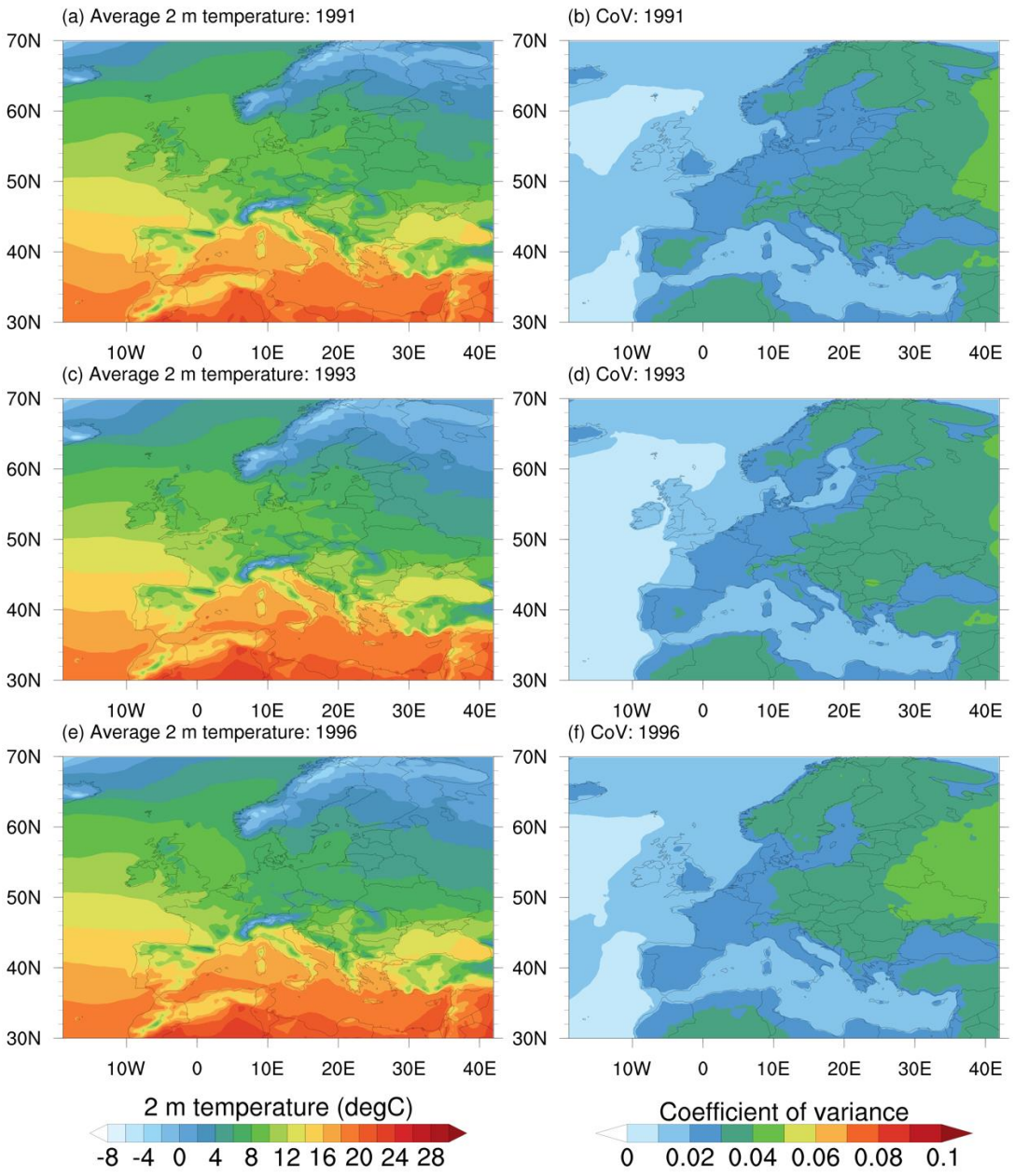

Figure 35: (a-e) Mean and (b-f) coefficient of variation of hourly 2 m temperature during cool years (a-b) 1991, (c-d) 1993, and (e-f) 1996.

Finally, the 2 m temperature statistics are analyzed on a seasonal time scale to understand the influence of different seasons, as presented in Figure 36. From the figure, it is evident that the 2 m temperature is maximum during summer as expected and minimum during winter. Over Europe, the temperature plunges from 17 °C during summer to -3 °C during winter. Throughout all the seasons, the Mediterranean Sea acts as a heat sink and provides necessary heat to the surrounding countries. During autumn, the coefficient of variation is higher than the overall, indicating the temperatures seem to fluctuate

This project has received funding from the Europeans Union's Horizon 2020 research & innovation programme under grant agreement number 101036457.

considerable. Similarly, the coefficient of variation during summer is very less, indicating little to no fluctuations in the temperature.

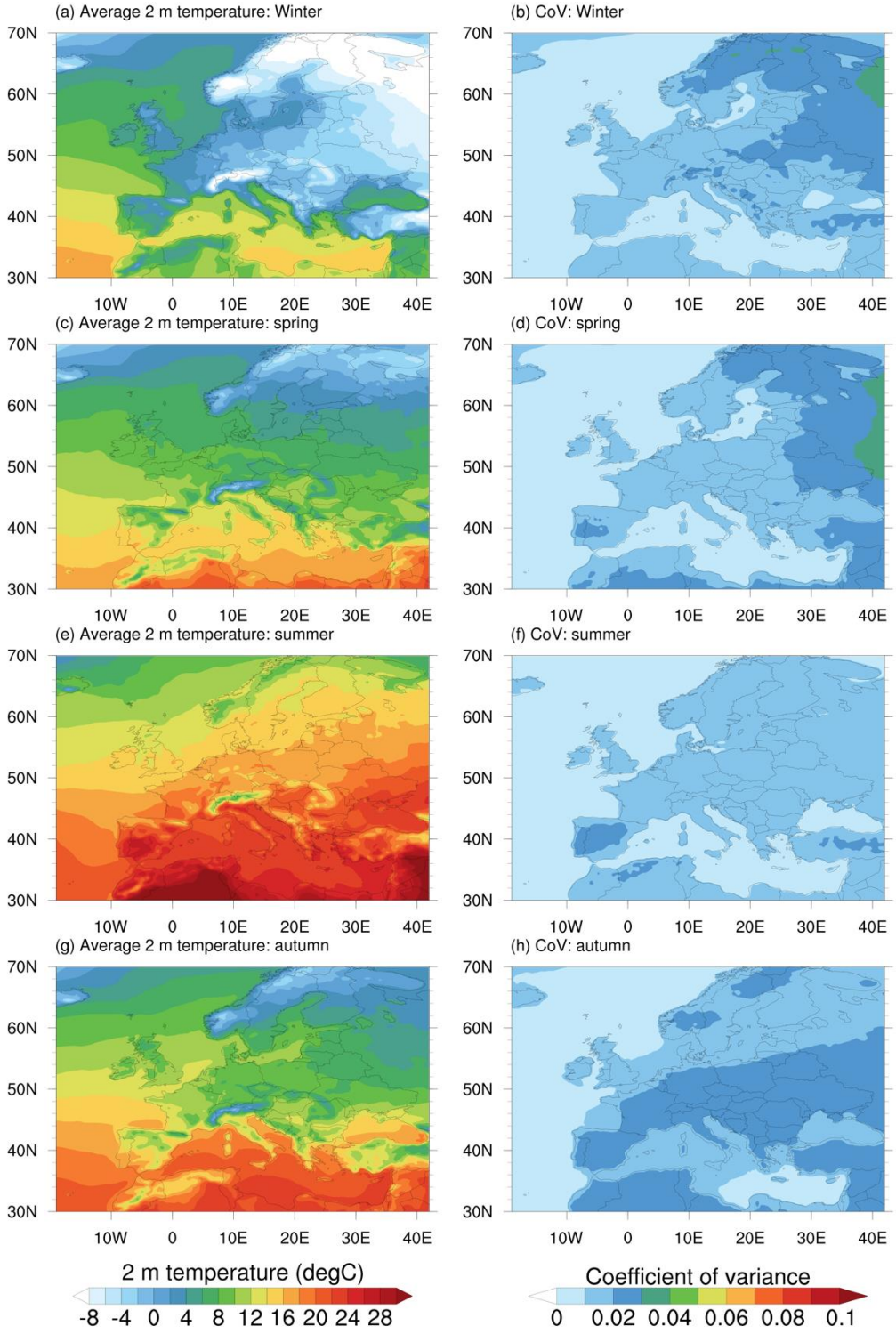

Figure 36: (a-g) Mean and (b-h) coefficient of variation of hourly 2 m temperature during seasons (a-b) winter, (c-d) spring, (e-f) summer, and (g-h) autumn.

This project has received funding from the Europeans Union's Horizon 2020 research & innovation programme under grant agreement number 101036457.

6.2 Solar power assessment

A preliminary study of solar energy coarse map assessment over Europe is conducted using the ERA5 reanalysis Surface Solar Radiation Downward (SSRD) variable. The assessment is conducted for a period of 30 years from 1990 to 2020, at hourly, seasonal, yearly, and overall time scales. The surface solar radiation at the four locations mentioned in Figure 14 is binned at 20 W/m2 intervals and their histograms are visualized in Figure 37. From the figure, it is evident that the surface solar radiation follows an exponential distribution, rather than a normal distribution.

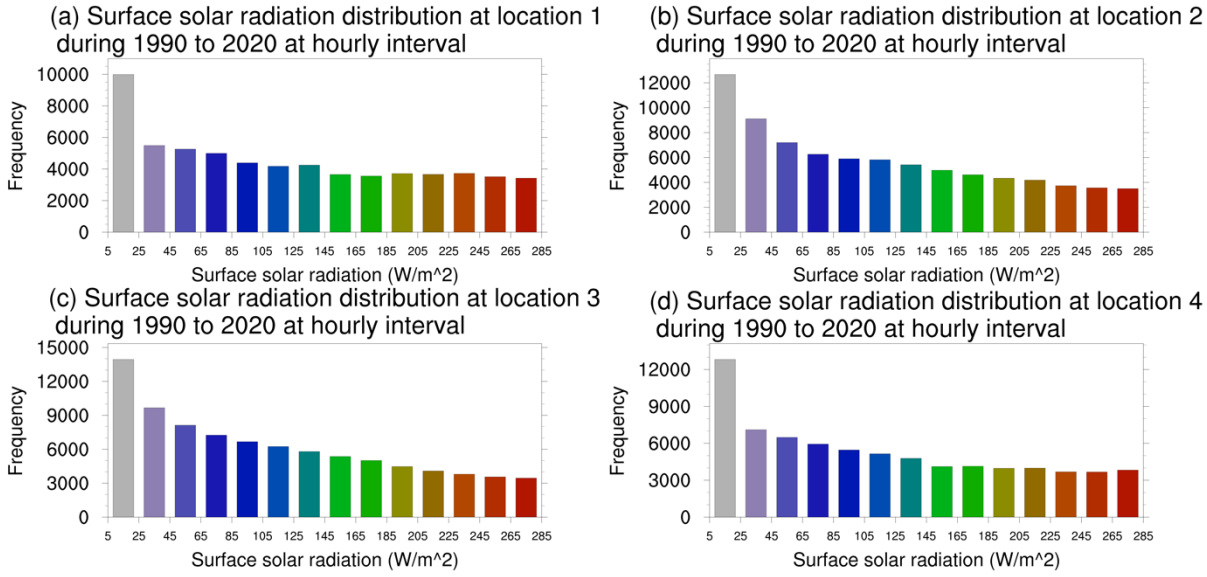

Figure 37: Histograms of surface solar radiation at locations (a) Gulf of Lion, (b) coast of Belgium, (c) coast of Ireland, and (d) Bay of Biscay.

Figure 38 shows the overall mean and coefficient of variance of surface solar radiation during 1990 to 2020. From figure, it is evident that the North Sea receives 140 W/m2 solar radiation and the west coast of Ireland receives 130 W/m2, but the variation is high, which is around 1.55. In contrast, the west coast of Portugal and the coastal regions around the Mediterranean Sea receive roughly 200 W/m2 solar radiation with lower variability than the North Sea. The polar region beyond 60 N receives approximately 70 W/m2 solar radiation with a large variability above 1.6, implying not being suitable for solar energy production. These variations are attributed to the distance from Earth's equator, which in turn influences the number of daytime hours over a specific region. Thus, examining the solar radiation at every hour might give an understanding of the available energy.

This project has received funding from the Europeans Union's Horizon 2020 research & innovation programme under grant agreement number 101036457.

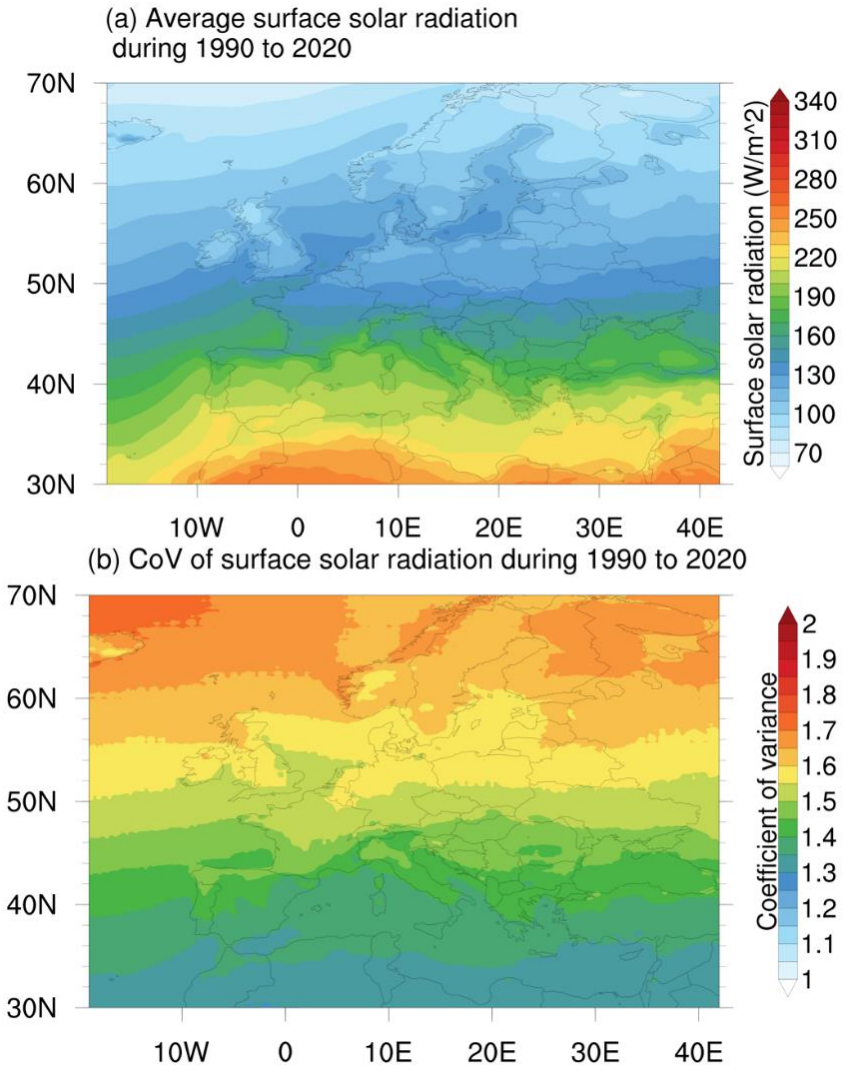

Figure 38: (a) Mean and (b) coefficient of variation of hourly surface solar radiation from 1990 to 2020.

Figure 39 shows the surface solar radiation at every 2 hours averaged over 1990 to 2020, which clearly illustrates the solar radiation available at every hour. The North Sea, the west coast of Ireland, and the coast of Belgium receive solar radiation higher than 100 W/m^2 from 0800 UTC to 1800 UTC hours, and during 1000 to 1400 UTC hours the solar radiation reach is above 340 W/m^2. In contrast, the west coast of Portugal receives much higher solar radiation compared to the three locations, and that too for 11 hours. This makes the west coast of Portugal more suitable for solar power production.

This project has received funding from the Europeans Union's Horizon 2020 research & innovation programme under grant agreement number 101036457.

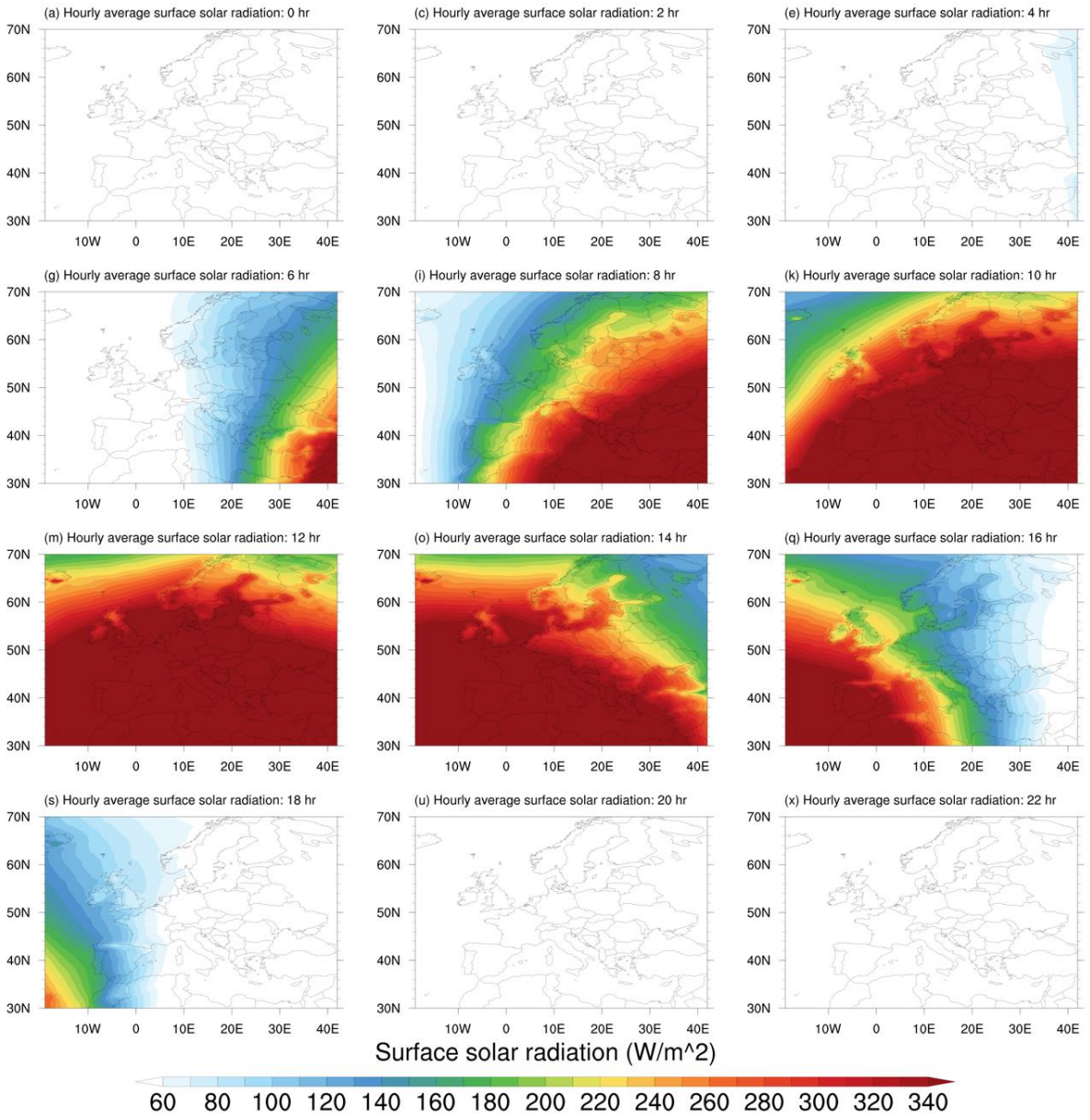

Figure 39: Mean hourly surface solar radiation averaged at every hour from 1990 to 2020.

In addition, the peak and low energy years are identified based on the percentage deviation of annual mean solar radiation about that of the overall 30 years mean, as given in Equation 9. Figure 40 until Figure 42 show the yearly mean solar radiation deviation for years 1990 to 2020. From these figures, it is evident that the mean solar radiation during 2003, 2018, and 2020 is higher than the overall mean by 8% to 9%, over the majority of the area.

These years are considered as peak energy years. In contrast, the mean solar radiation during 1991, 1996, and 1998 is lower than the overall mean by 8% to 10%, over majority of the area.

This project has received funding from the Europeans Union's Horizon 2020 research & innovation programme under grant agreement number 101036457.

These years are considered as the low energy years. A close observation of Figure 38, Figure 39, and Figure 40 reveals the polar region show extreme deviations compared to the 30 years mean. However, these fluctuations are close to 5-7 W/m^2, since the polar region receives less than 70 W/m2 on average.

This project has received funding from the Europeans Union's Horizon 2020 research & innovation programme under grant agreement number 101036457.

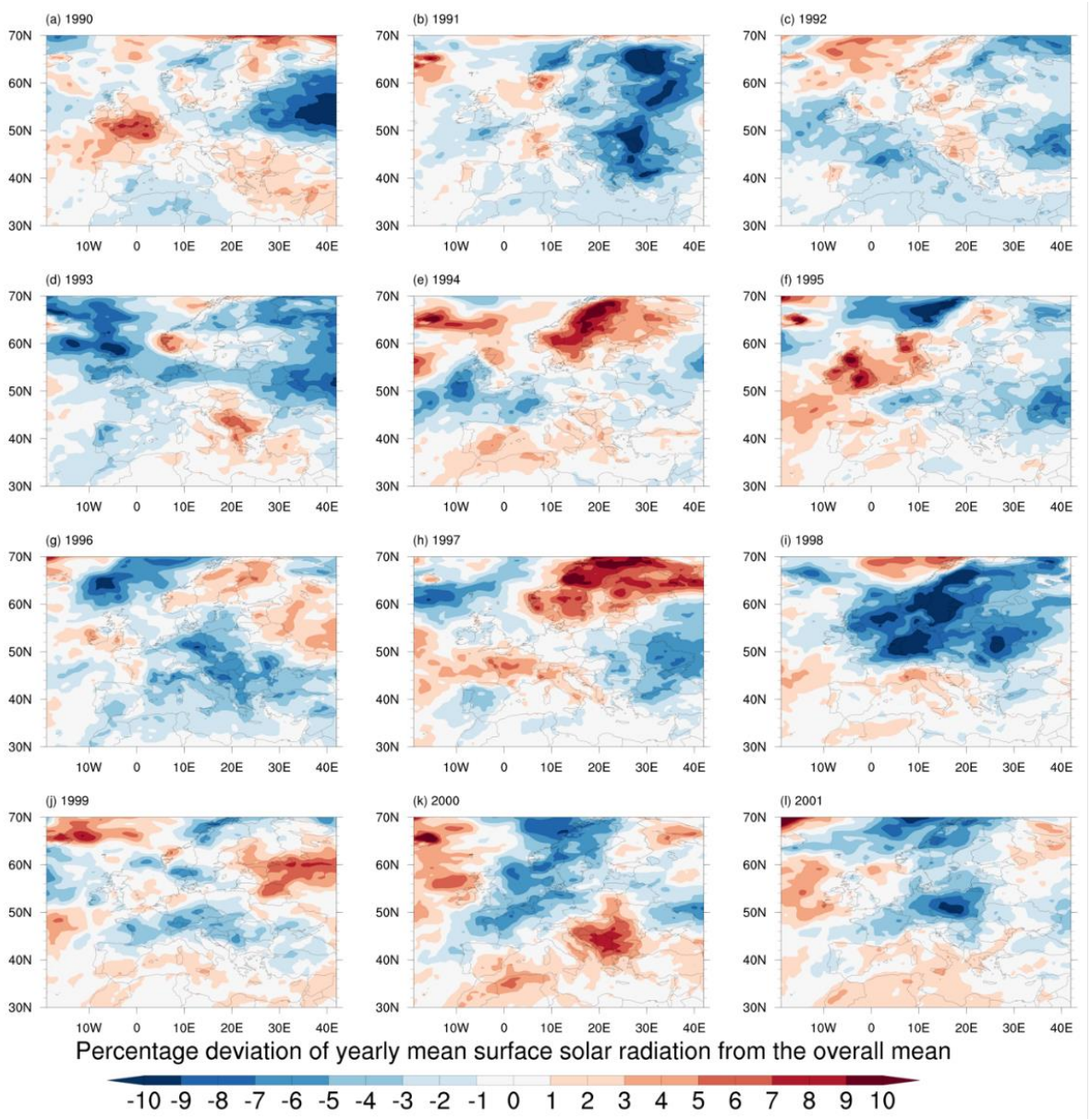

Figure 40: Yearly mean surface solar radiation deviation from overall mean.

This project has received funding from the Europeans Union's Horizon 2020 research & innovation programme under grant agreement number 101036457.

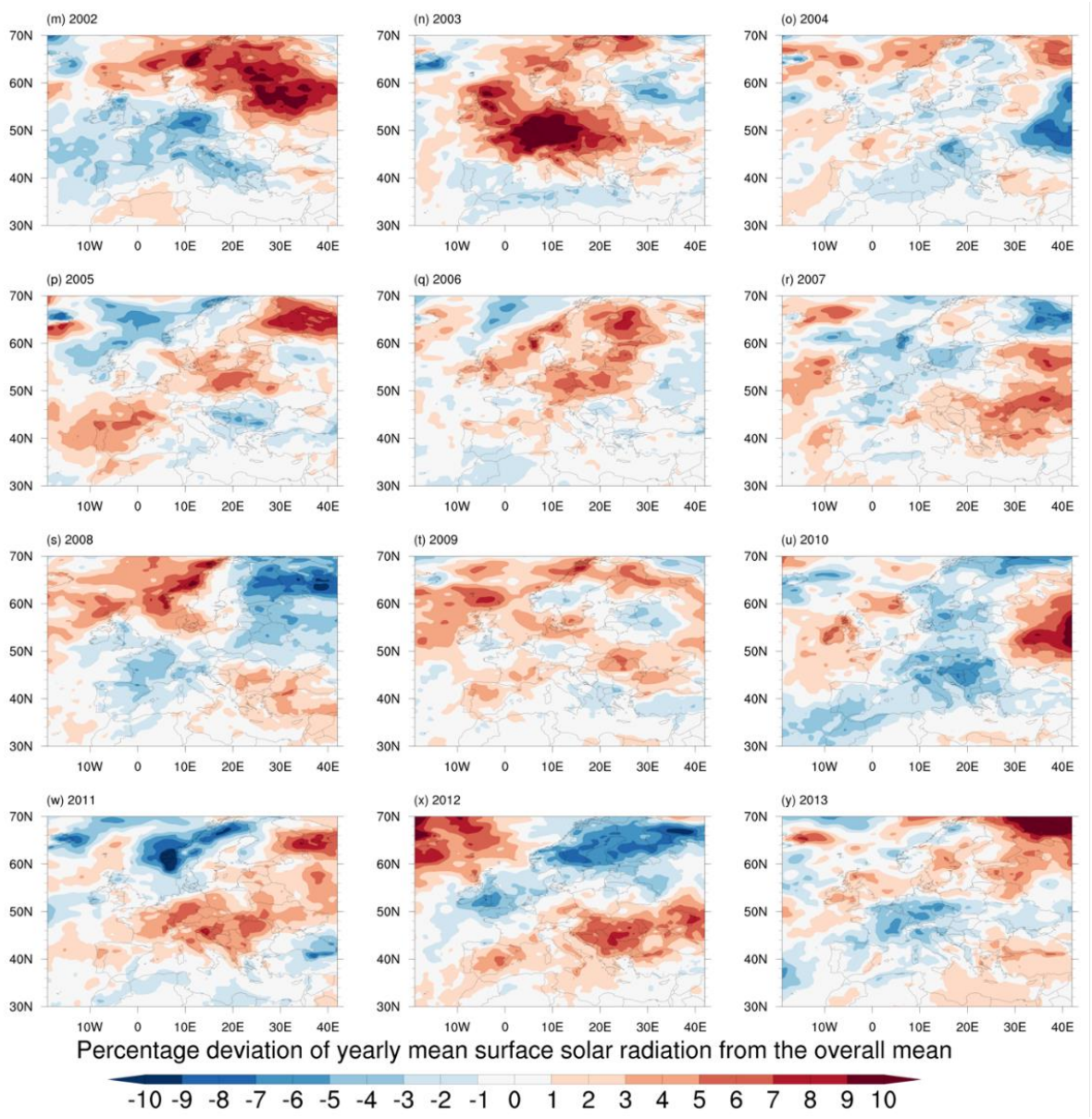

Figure 41: Yearly mean surface solar radiation deviation from overall mean (Continuation)

This project has received funding from the Europeans Union's Horizon 2020 research & innovation programme under grant agreement number 101036457.

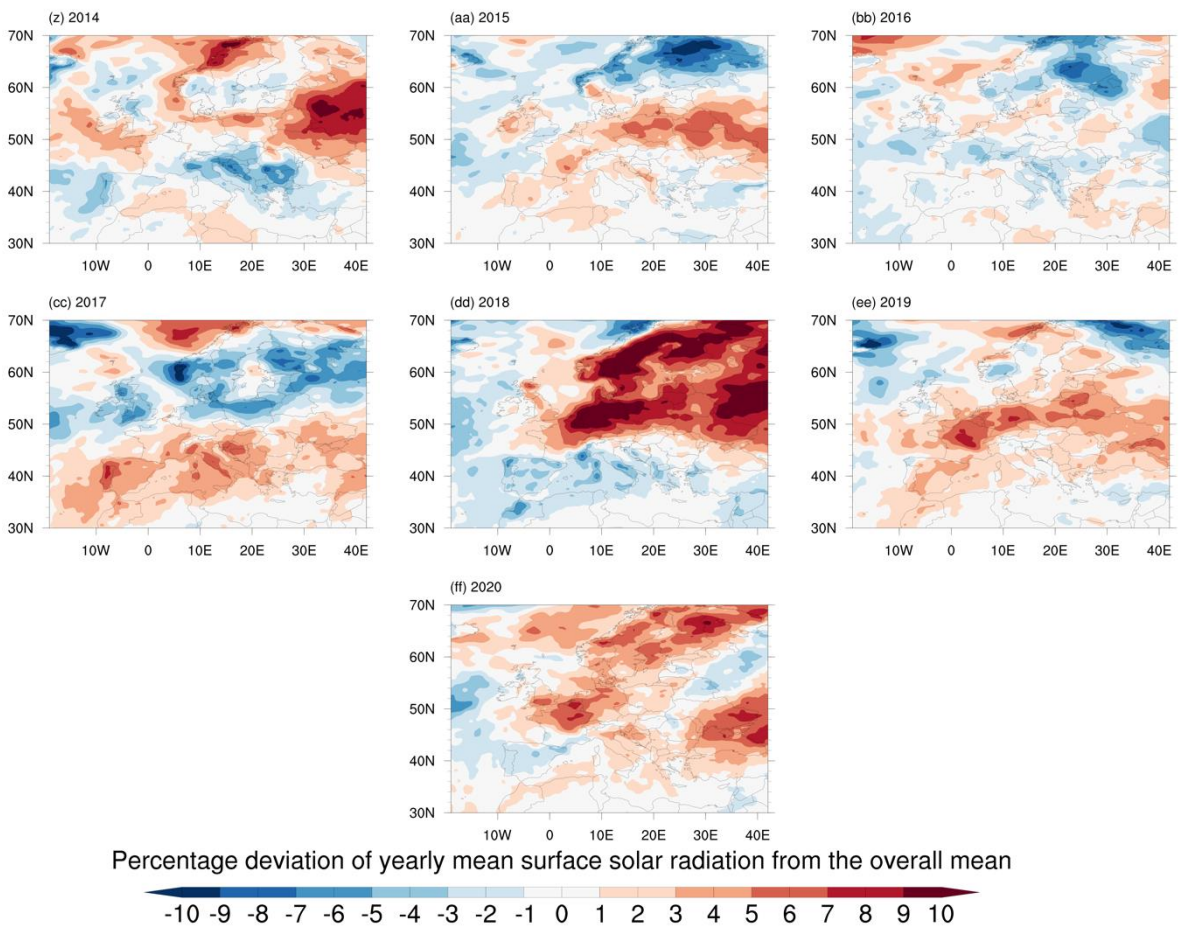

Figure 42: Yearly mean surface solar radiation deviation from overall mean (Continuation)

Figure 43 and Figure 44 illustrate the solar radiation characteristics for peak and low energy years. During the peak energy years, the North Sea receives 150 W/m^2 solar radiation with a coefficient of variability of 1.55, and the coast of Ireland receive 140 W/m^2 solar radiation with a similar variability. It is to be noted that the difference between the mean and peak radiation is merely 10 W/m^2, which itself is not uniform throughout the region.

During the low energy years, the same areas receive at least an order of 10 W/m^2 lower radiation than the mean. In contrast, the west coast of Portugal and the Mediterranean Sea receive similar radiation during the low peak energy years with little to no difference in their variability. This also strengthens the assumption that the west coast of Portugal is more suitable for solar farms. Apart from the mean radiation, the variability characteristics are fairly similar during the peak and low wind years if we look at it as a whole. To understand the characteristics in detail, further analysis is needed by selecting specific locations.

This project has received funding from the Europeans Union's Horizon 2020 research & innovation programme under grant agreement number 101036457.

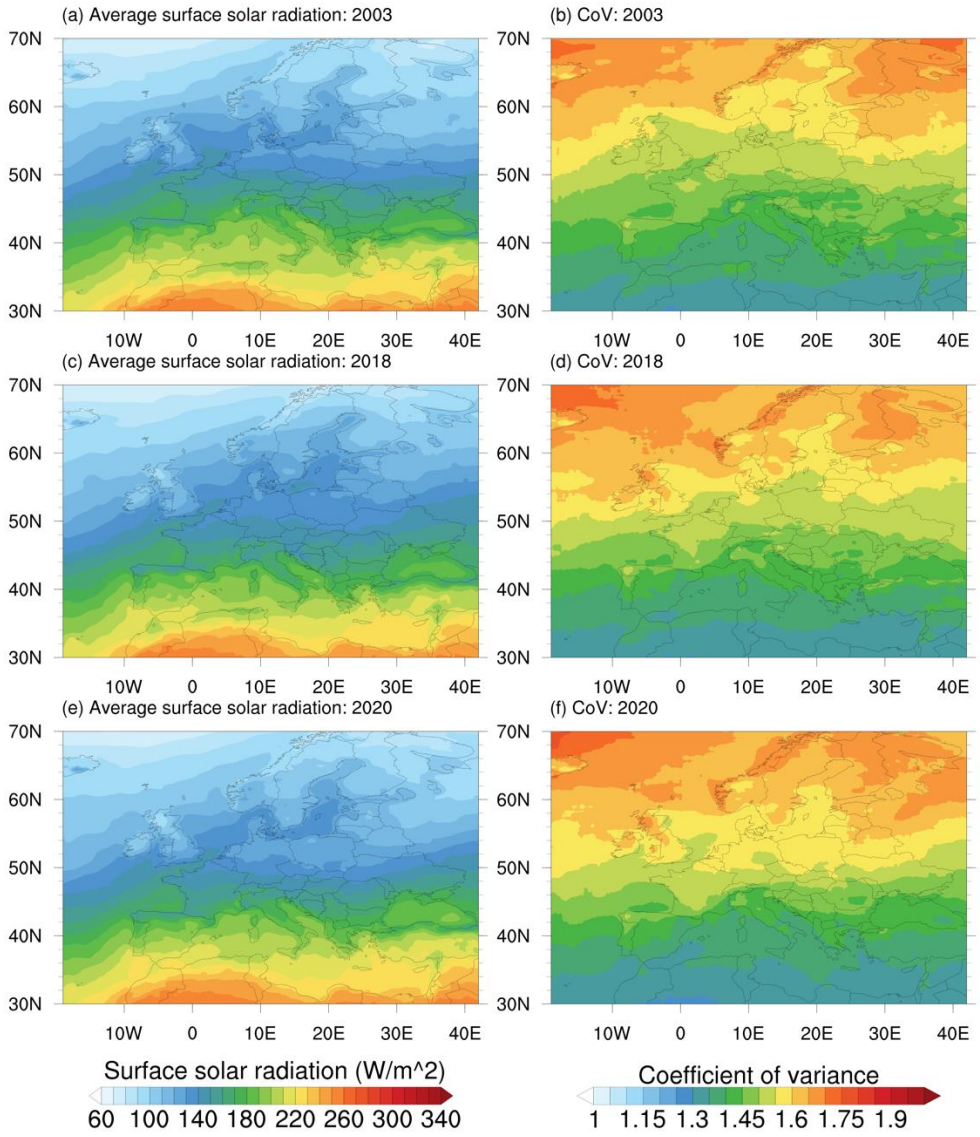

Figure 43: (a-e) Mean and (b-f) coefficient of variation of hourly surface solar radiation during peak energy years (a-b) 2003, (c-d) 2018, and (e-f) 2020.

This project has received funding from the Europeans Union's Horizon 2020 research & innovation programme under grant agreement number 101036457.

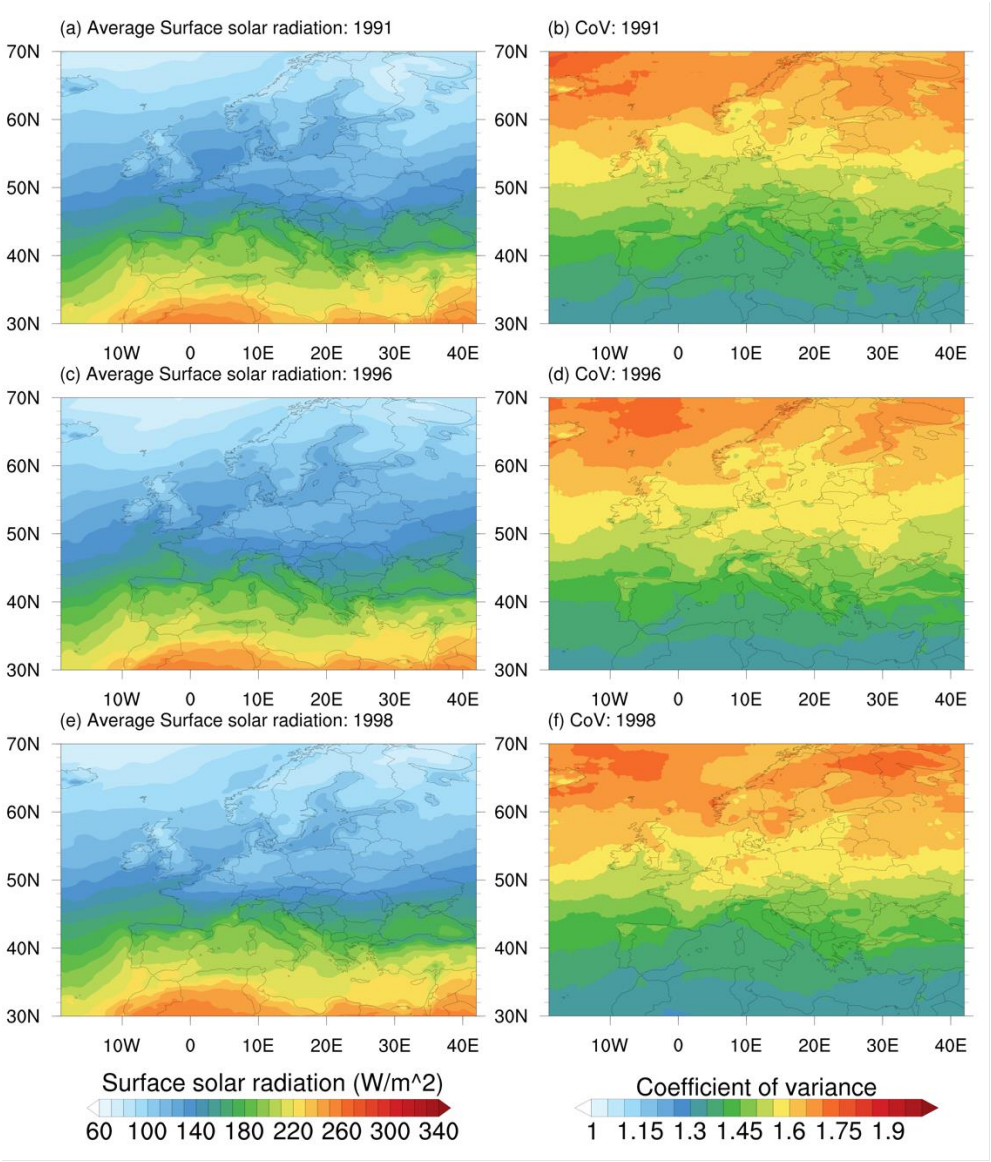

Figure 44: (a-e) Mean and (b-f) coefficient of variation of hourly surface solar radiation during low energy years (a-b) 1991, (c-d) 1996, and (e-f) 1998.

Finally, the solar radiation statistics are analysed on a seasonal time scale to understand the influence of different seasons, as presented in Figure 45. From the figure, it is evident that the solar radiation is maximum during summer as expected and minimum during winter.

The North Sea and the west coast of Ireland receive little to no solar radiation autumn and winter, whereas the west coast of Portugal receives higher than 110 W/m^2 throughout all the seasons. Even though in summer, the North Sea receives more solar radiation around 240 W/m^2 compared to the west coast of Ireland, which receives around 200 W/m^2. In addition, variability in solar radiation over the North Sea and the west coast of Ireland is maximum during autumn and spring, whereas the

This project has received funding from the Europeans Union's Horizon 2020 research & innovation programme under grant agreement number 101036457.

variability in solar radiation over the west coast of Portugal is highest in winter and least in summer.

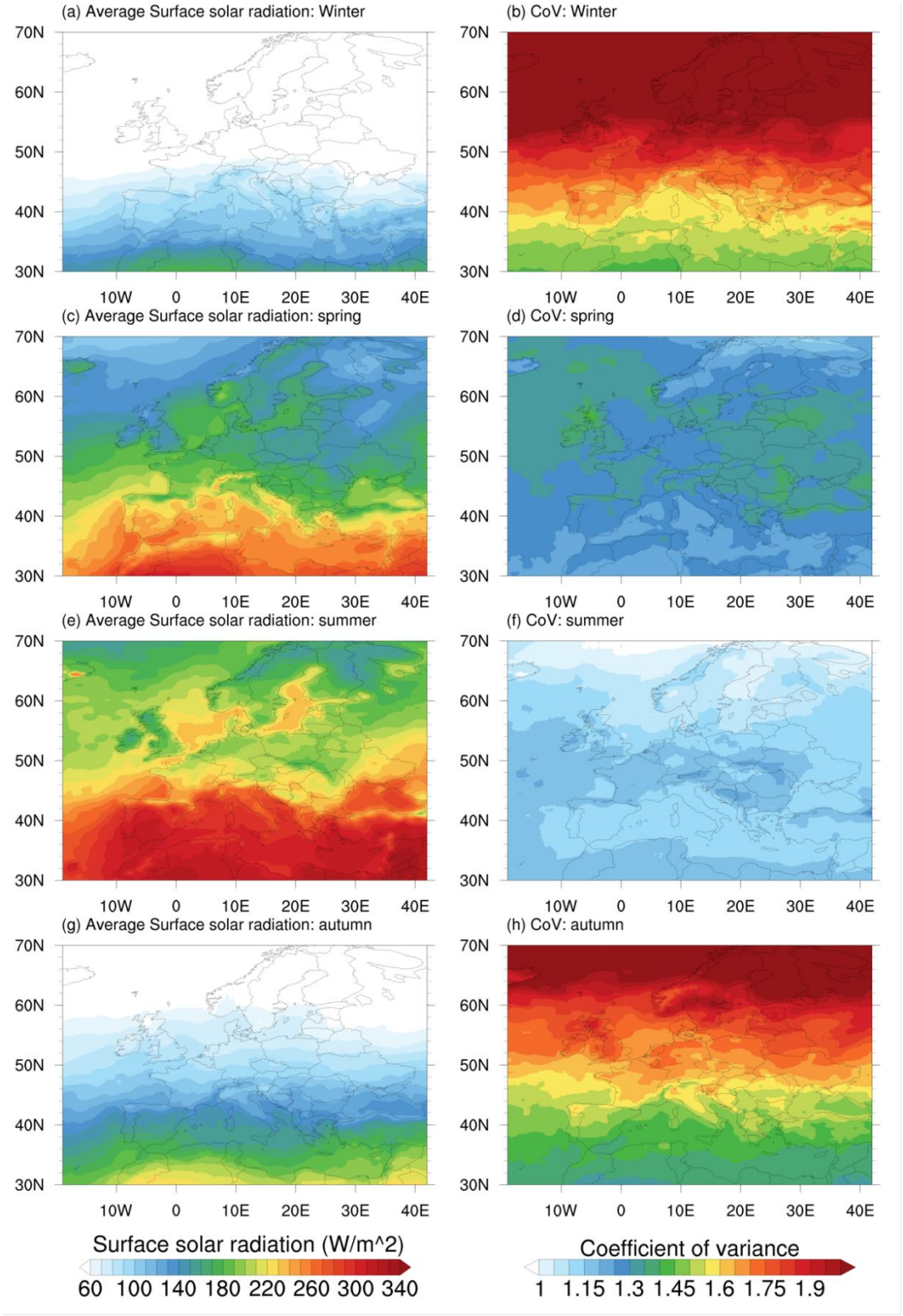

Figure 45: (a-g) Mean and (b-h) coefficient of variation of hourly surface solar radiation during seasons (a-b) winter, (c-d) spring, (e-f) summer, and (g-h) autumn.

This project has received funding from the Europeans Union's Horizon 2020 research & innovation programme under grant agreement number 101036457.

7 Summary

This report analysed 30 years of coarse data in order to provide a comprehensive preliminary overview; of the renewable potential for wind-wave-solar over the European continent.

The long-term nature of the datasets allowed us to perform a comprehensive energy and climate analysis. While, our primary focus was to quantify the energy potentials, we also assessed the persistence and expected variance of wind-solar-wave renewable resources.

The analysis provides several outcomes, but some key findings are

For wave and wave energy (predominately for deep waters)

- ✓ The seasonal average for the 30 years period shows the expected overall increase of wave heights and periods along the Atlantic coasts, with Portugal and Scotland experiencing consistently mean conditions above 5 m
- ✓ Coefficient of Variation (CoV) is higher (>0.6) at areas where wave conditions are mostly driven by local winds (local wave generation), with Portugal having low CoV while maintaining high energy density
- ✓ Mean wave energy density at higher latitudes in above 56 kW/m, in the North Sea above 10 kW/m and in the South Atlantic coastlines of Europe above 35 kW/m

For wind speeds and wind energy at 100m vertical height

- ✓ The average wind speed over the north sea is above 10 m/s, with a low CoV (0.2), Southern European Atlantic coastlines have 8 m/s mean wind speeds but with higher variability.
- ✓ Mean Wind energy density over the North Sea at 100m vertical level is 1100 W/m2, Ireland is 1300 W/m2 and Portugal 600 W/m2

For Solar radiation on surface, and ambient temperatures

- ✓ European mean temperature over 30 years is approximately 27 °C with low variability
- ✓ Mean solar energy density over North Sea is 140 W/m2, Ireland 130 W/m2, and throughout Southern Europe over 190 W/m2

This project has received funding from the Europeans Union's Horizon 2020 research & innovation programme under grant agreement number 101036457.

8 Bibliography

The WAVEWATCH III® Development Group, 2019. *User Manual and System Documentation,* s.l.: s.n.

Alday, M., Accensi, M., Ardhuin, F. & Dodet, G., 2021. A global wave parameter database for geophysical applications. Part 3: Improved forcing and spectral resolution. *Ocean Modelling,* Volume 166, p. 101848.

Alday, M., Ardhuin, F., Dodet, G. & Accensi, M., 2022. Accuracy of numerical wave model results: application to the Atlantic coasts of Europe. *Ocean Science,* 18(6), pp. 1665--1689.

Ardhuin, F., Herbers, T. H. C., Vledder, G. P. v. & Watts, K. P., 2007. Swell and Slanting-Fetch Effects on Wind Wave Growth. *Journal of Physical Oceanography,* Volume 37, pp. 908--931.

Ardhuin, F. et al., 2010. Semiempirical Dissipation Source Functions for Ocean Waves. Part I: Definition, Calibration, and Validation. *Journal of Physical Oceanography,* Volume 40, pp. 1917--1941.

Booij, N., Holthuijsen, L. H. & Ris, R. C., 1997. The" SWAN" wave model for shallow water. In: *Coastal Engineering 1996.* s.l.:s.n., pp. 668-676.

Cavaleri, L. & Bertolli, L., 1997. n search of the correct wind and wave fields in a minor basin. *Monthly weather review,* Volume 125, pp. 1964--1975.

Cavaleri, L., Bertotti, L. & Pezzutto, P., 2019. Accuracy of altimeter data in inner and coastal seas. *Ocean Science.*

Dobson, F., Perrie, W. & Toulany, B., 1989. On the deep-water fetch laws for wind-generated surface gravity waves. *Atmosphere-Ocean,* Volume 27, pp. 210--236.

Girard-Ardhuin, F. & Ezraty, R., 2012. Enhanced Arctic sea ice drift estimation merging radiometer and scatterometer data. *IEEE Transactions on Geoscience and Remote Sensing,* 50(7), pp. 2639--2648.

Guillou, N., 2014. Wave-energy dissipation by bottom friction in the English Channel. *Ocean Enginnering,* Volume 82, pp. 42--51.

Guillou, N., Lavidas, G. & Chapalain, G., 2020. Wave Energy Resource Assessment for Exploitation—A Review. *Journal of Marine Science and Engineering.*

Hersbach, H. et al., 2020. The ERA5 global reanalysis. *Quarterly Journal of the Royal Meteorological Society,* Volume 146, pp. 1999--2049.

Lavidas, G., Polinder & henk, 2019. North Sea Wave Database (NSWD) and the Need for Reliable Resource Data: A 38 Year Database for

This project has received funding from the Europeans Union's Horizon 2020 research & innovation programme under grant agreement number 101036457.

Metocean and Wave Energy Assessments. *Journal of Marine Science and Engineering.*

Lavidas, G. & Vengatesan, V., 2018. Application of numerical wave models at European coastlines: A review. *Renewable and Sustainable Energy Reviews,* Volume 92, pp. 489-500.

Li, B., Basu, S., Watson, S. & Russchenberg, H. W., 2021. Mesoscale modelling of a "Dukeflaute" event. *Wind Energy,* Volume 24, pp. 5-23.

Mulet, S. et al., 2021. The new CNES-CLS18 global mean dynamic topography. *Ocean Science,* 17(3), pp. 789--808.

Piollé, J.-F.et al., 2022. ESA Sea State Climate Change Initiative (Sea State cci): Global remote sensing multi-mission along-track significant wave height from altimetry, L2P product, version 3..

Rio, M.-H., Mulet, S. & Picot, N., 2014. Beyond GOCE for the ocean circulation estimate: Synergetic use of altimetry, gravimetry, and in situ data provides new insight into geostrophic and Ekman currents. *Geophysical Research Letters,* 41(24), pp. 8918--8925.

Rivas, M. B. & Stoffelen, A., 2019. Characterizing ERA-Interim and ERA5 surface wind biases using {ASCAT}. *Ocean Science,* Volume 15, pp. 831--852.

This project has received funding from the Europeans Union's Horizon 2020 research & innovation programme under grant agreement number 101036457.